Diacylglycerol kinase δ and sphingomyelin synthase–related protein functionally interact via their sterile α motif domains

Received for publication, December 17, 2019, and in revised form, January 23, 2020 Published, Papers in Press, January 24, 2020, DOI 10.1074/jbc.RA119.012369

Chiaki Murakami[‡], Fumi Hoshino[‡], Hiromichi Sakai[§], Yasuhiro Hayashi[¶], Atsushi Yamashita[¶], and Fumio Sakane[‡1]

From the [‡]Department of Chemistry, Graduate School of Science, Chiba University, Chiba 263-8522, Japan, the [§]Department of Biosignaling and Radioisotope Experiment, Interdisciplinary Center for Science Research, Organization for Research and Academic Information, Shimane University, Izumo 693-8501, Japan, and the [¶]Faculty of Pharma Sciences, Teikyo University, Kaga 2-11-1, Itabashi-ku, Tokyo 173-8605, Japan

Edited by Qi-Qun Tang

The δ isozyme of diacylglycerol kinase (DGKδ) plays critical roles in lipid signaling by converting diacylglycerol (DG) to phosphatidic acid (PA). We previously demonstrated that DGKδ preferably phosphorylates palmitic acid (16:0)- and/or palmitoleic acid (16:1)-containing DG molecular species, but not arachidonic acid (20:4)-containing DG species, which are recognized as DGK substrates derived from phosphatidylinositol turnover, in high glucose-stimulated myoblasts. However, little is known about the origin of these DG molecular species. DGKδ and two DG-generating enzymes, sphingomyelin synthase (SMS) 1 and SMS-related protein (SMSr), contain a sterile α motif domain (SAMD). In this study, we found that SMSr–SAMD, but not SMS1–SAMD, co-immunoprecipitates with DGKδ–SAMD. Full-length DGKδ co-precipitated with full-length SMSr more strongly than with SMS1. However, SAMD-deleted variants of SMSr and DGKδ interacted only weakly with full-length DGKδ and SMSr, respectively. These results strongly suggested that DGKδ interacts with SMSr through their respective SAMDs. To determine the functional outcomes of the relationship between DGKδ and SMSr, we used LC-MS/MS to investigate whether overexpression of DGKδ and/or SMSr in COS-7 cells alters the levels of PA species. We found that SMSr overexpression significantly enhances the production of 16:0- or 16:1-containing PA species such as 14:0/16:0-, 16:0/16:0-, 16:0/18:1-, and/or 16:1/18:1-PA in DGKδ-overexpressing COS-7 cells. Moreover, SMSr enhanced DGKδ activity via their SAMDs *in vitro*. Taken together, these results strongly suggest that SMSr is a candidate DG-providing enzyme upstream of DGKδ and that the two enzymes represent a new pathway independent of phosphatidylinositol turnover.

Diacylglycerol kinase (DGK)[2] utilizes diacylglycerol (DG) as a substrate to generate phosphatidic acid (PA) (1–5). Ten mammalian DGK isozymes (α, β, γ, δ, ε, ζ, η, θ, ι, and κ) have been identified to date and are categorized into five groups (types I–V) based on their structural features. Because DG and PA act as lipid second messengers, DGK plays important roles in signal transductions of a wide variety of physiological and pathological events by controlling the balance between DG and PA. For example, DG is a well-established bioactive lipid that activates protein kinase C (PKC) (6) and Ras guanyl nucleotide–releasing protein (7). It is known that accumulation of DG induces insulin resistance by activation of PKC isoforms (8–12), which phosphorylate and inactivate insulin receptor substrate-1 and, consequently, attenuate insulin-stimulated tyrosine phosphorylation of insulin receptor substrate-1 (13). Chibalin *et al.* (14) reported that the expression levels of DGKδ (type II isozyme) (Fig. 1*A*) and its activities are decreased in skeletal muscles from type 2 diabetic patients, indicating that the decrease of DGKδ protein is closely related to the pathogenesis of type 2 diabetes. Moreover, we determined that DGKδ primarily utilizes palmitic acid (16:0)- and/or palmitoleic acid (16:1)-containing DG molecular species, such as 14:0/16:0-, 14:0/16:1-, 16:0/16:0-, 16:0/16:1-, 16:0/18:0-, and 16:0/18:1-DG species (*X:Y* = the total number of carbon atoms:the total number of double bonds in the fatty acyl moiety of glycerol backbone), but not arachidonic acid (20:4)-containing DG species generally recognized as DGK substrates and derived from phosphatidylinositol (PI) turnover, in high-glucose–stimulated C2C12 myoblasts (1, 15). However, the upstream pathway of DGKδ remains unclear.

Type II DGKs consist of the δ1, δ2, η1, η2, and κ isoforms (Fig. 1*A*). DGKs δ1, δ2, and η2 have a sterile α motif domain

This work was supported in part by MEXT/JSPS KAKENHI Grants JP18J20003 (to C. M.) and 25116704, 26291017, 17H03650, and 15K14470 (to F. S.), Japan Science and Technology Agency Grants AS251Z01788Q and AS2621643Q (to F. S.), the Futaba Electronic Memorial Foundation (to F. S.), the Ono Medical Research Foundation (to F. S.), the Japan Foundation for Applied Enzymology (to F. S.), the Food Science Institute Foundation (to F. S.), the Skylark Food Science Institute to (F. S.), the Hamaguchi Foundation for the Advancement of Biochemistry (to F. S.), the Daiichi-Sankyo Foundation of Life Science (to F. S.), the Terumo Life Science Foundation (to F. S.), the Asahi Group Foundation (to F. S.), the Japan Milk Academic Alliance (to F. S.), the Japan Food Chemical Research Foundation (to F. S.), and the SENSHIN Medical Research Foundation (to F. S.). The authors declare that they have no conflicts of interest with the contents of this article.

This article contains Tables S1 and S2.

[1] To whom correspondence should be addressed. Tel./Fax: 81-43-290-3695; E-mail: sakane@faculty.chiba-u.jp.

[2] The abbreviations used are: DGK, diacylglycerol kinase; DGKδ, diacylglycerol kinase δ isozyme; DG, diacylglycerol; ER, endoplasmic reticulum; PA, phosphatidic acid; PC, phosphatidylcholine; PE; phosphatidylethanolamine; PLC, phospholipase C; SMS, sphingomyelin synthase; SMSr, sphingomyelin synthase-related protein; SAMD, sterile α motif domain; IP, immunoprecipitation; IPTG, isopropyl 1-thio-β-D-galactopyranoside; TF, trigger factor; FBS, fetal bovine serum; PMSF, phenylmethylsulfonyl fluoride; PI, phosphatidylinositol; GST, GSH *S*-transferase.

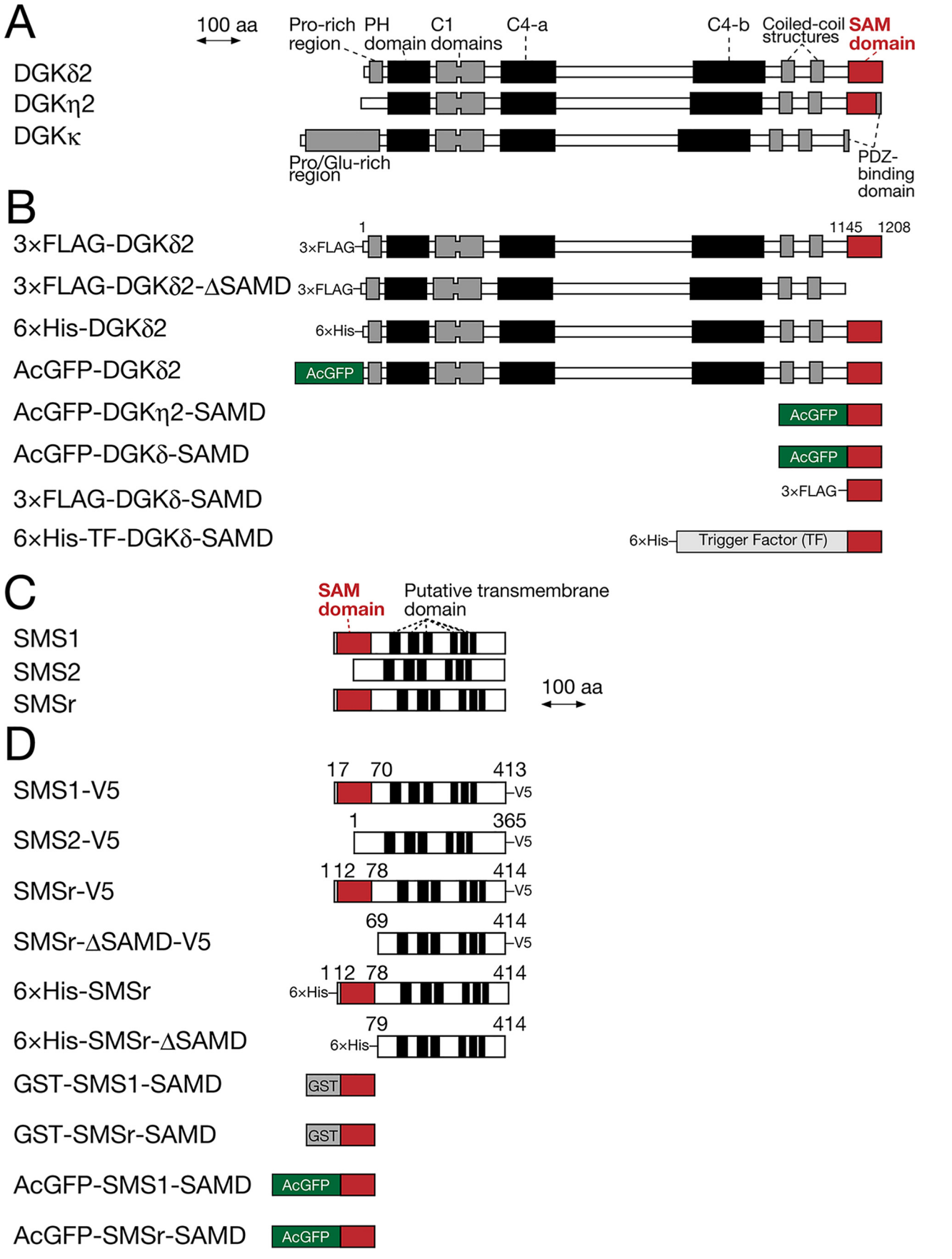
A
100 aa
Pro-rich region
PH domain
C1 domains
C4-a
C4-b
Coiled-coil structures
SAM domain
DGKδ2
DGKη2
DGKκ
Pro/Glu-rich region
PDZ-binding domain
B
1
1145
1208
3×FLAG-DGKδ2
3×FLAG-DGKδ2-ΔSAMD
6×His-DGKδ2
AcGFP-DGKδ2
AcGFP-DGKη2-SAMD
AcGFP-DGKδ-SAMD
3×FLAG-DGKδ-SAMD
6×His-TF-DGKδ-SAMD
3×FLAG
6×His
AcGFP
Trigger Factor (TF)
C
SAM domain
Putative transmembrane domain
SMS1
SMS2
SMSr
100 aa
D
SMS1-V5
SMS2-V5
SMSr-V5
SMSr-ΔSAMD-V5
6×His-SMSr
6×His-SMSr-ΔSAMD
GST-SMS1-SAMD
GST-SMSr-SAMD
AcGFP-SMS1-SAMD
AcGFP-SMSr-SAMD
17
70
413
1
365
112
78
414
69
79
V5
GST

A

B

	DGKη-SAMD	SMSr-SAMD	SMS1-SAMD
DGKδ-SAMD	82.8%	32.8%	27.5%
DGKη-SAMD		34.3%	27.3%
SMSr-SAMD			30.9%

Figure 2. Multiple sequence alignment of the SAMDs of DGKδ2, DGKη2, SMSr, and SMS1. *A,* multiple sequence alignment of the human SAMDs of DGKδ2, DGKη2, SMSr, and SMS1. Multiple sequence alignment was created using ClustalW (version 2.1) (51, 52) provided from the DNA Data Bank of Japan (DDBJ). The following were used: human DGKδ–SAMD (Uniprot, Q16760-1; amino acid residues, 1145–1208); human DGKη2–SAMD (Uniprot, Q86XP1-1, amino acid residues, 1151–1214); human SMSr–SAMD (Uniprot, Q96LT4; amino acid residues, 12–78); and human SMS1–SAMD (Uniprot, Q86VZ5; amino acid residues, 7–70). Note that all residues of SMSr–SAMD and DGKδ–SAMD are fully conserved in mouse and human. *Hyphens* show gaps inserted to achieve maximum alignment. Compared with DGKδ–SAMD, *white letters on black background* indicate fully-conserved residues, and *black letters on gray background* indicate strongly similar residues (scoring >0.5 in the Gonnet PAM 250 matrix). The residues marked with an *asterisk* are critical for homo-oligomerization of DGKδ–SAMD (25). *B,* amino acid identities between human SAMDs of DGKδ2, DGKη2, SMSr, and SMS1. Amino acid identity was determined using Pairwise Sequence Alignment provided by the European Molecular Biology Open Software Suite (EMBOSS).

(SAMD) at their C termini. A SAMD is one of the most common protein modules found in eukaryotic genomes and forms a homodimer. SAMDs are remarkably versatile in their binding partners, including other cognate SAMDs, RNA (16), and lipids (17). We reported that DGKδ1, DGKδ2, and DGKη2 can form homo- and heterodimeric structures, as well as dimeric–tetrameric complexes, through their SAMDs *in vitro* and in cells (18–21).

Cabukusta *et al.* (22, 23) recently pointed out that the SAMD of sphingomyelin synthase (SMS)-related protein (SMSr/SAMD8) (Fig. 1*C*), a family member of SMS, is primarily structurally similar to the DGKδ–SAMD and demonstrated that SMSr–SAMD formed a homodimer, which is a crucial determinant of the subcellular localization of SMSr. SMSr is a six-transmembrane protein in the endoplasmic reticulum (ER), which generates DG by utilizing phosphatidylethanolamine (PE) and ceramide (24).

In this study, we investigated the interaction and functional relationship between DGKδ and SMSr because both proteins possess SAMDs, which are structurally similar to each other. Intriguingly, we found that DGKδ2 interacted and was functionally linked with SMSr via their SAMDs. Therefore, it is possible that SMSr is a DG-providing enzyme upstream of DGKδ and that these enzymes comprise a new pathway independent of PI turnover.

Results

DGKδ–SAMD interacted with SMSr–SAMD

We first compared the amino acid sequences of human DGKδ–SAMD, DGKη2–SAMD, SMS1–SAMD, and SMSr–SAMD using the ClustalW alignment tool (Fig. 2*A*). The residues marked with asterisks (Fig. 2*A*, *E31, D39, V48, G49,* and *K52*) are critical for DGKδ–SAMD homo-oligomerization as we reported previously (Fig. 2*A*) (25). The five residues were fully conserved in both the DGKδ–SAMD and DGKη2–SAMD (Fig. 2*A*). Interestingly, four of the five residues were conserved in the SMSr–SAMD (22). However, only one of the residues was conserved in the SMS1–SAMD. Moreover, we compared the SAMDs using pairwise sequence alignment (Fig. 2*B*). The results of pairwise comparisons showed that the SMSr–SAMD was more similar to the DGKδ–SAMD than the SMS1–SAMD (32.8% identity *versus* 27.5% identity). Interestingly, the identity between the SMSr–SAMD and the DGKδ–SAMD was higher than that between the SMSr–SAMD and the SMS1–SAMD (32.8% *versus* 30.9%) (Fig. 2). These results raised the possibility that SMSr and DGKδ formed heterodimeric complexes.

To investigate that possibility, we performed co-immunoprecipitation analysis using COS-7 cells co-expressing 3×FLAG-tagged DGKδ–SAMD and either AcGFP-tagged DGKδ–SAMD, DGKη2–SAMD, SMSr–SAMD, or SMS1–SAMD (Fig. 1, *B* and *D*). When the 3×FLAG-tagged DGKδ–SAMD was immunoprecipitated using an anti-FLAG antibody, AcGFP-tagged DGKδ–SAMD, DGKη2–SAMD, and SMSr–SAMD were co-immunoprecipitated with the 3×FLAG–DGKδ–SAMD (Fig. 3, *A* and *B*). However, AcGFP alone and AcGFP–SMS1–SAMD failed to be co-sedimented (Fig. 3, *A* and *B*). These results indicated that DGKδ–SAMD selectively associated with the SMSr–SAMD. The band intensity of the AcGFP–SMSr–SAMD precipitated with the 3×FLAG–DGKδ–SAMD was almost the same as that of the AcGFP–DGKδ–SAMD (Fig. 3, *A* and *B*), suggesting that the interaction affinity between SMSr–SAMD and DGKδ–SAMD was the same as that between the two DGKδ–SAMD proteins.

Figure 1. Protein structures of type II DGK and SMS isozymes and their mutants. *A,* structures of SAMD-containing type II DGK isozymes (δ2, η2, and κ). *C4-a*, N-terminal catalytic domain; *C4-b*, C-terminal catalytic domain; *PH*, pleckstrin homology domain. *B,* schematic representation of the DGKδ2 and DGKη2 constructs used in this study. *C,* structures of SMS1, SMS2, and SMSr. *D,* schematic representation of the SMSr and SMS1 constructs used in this study.

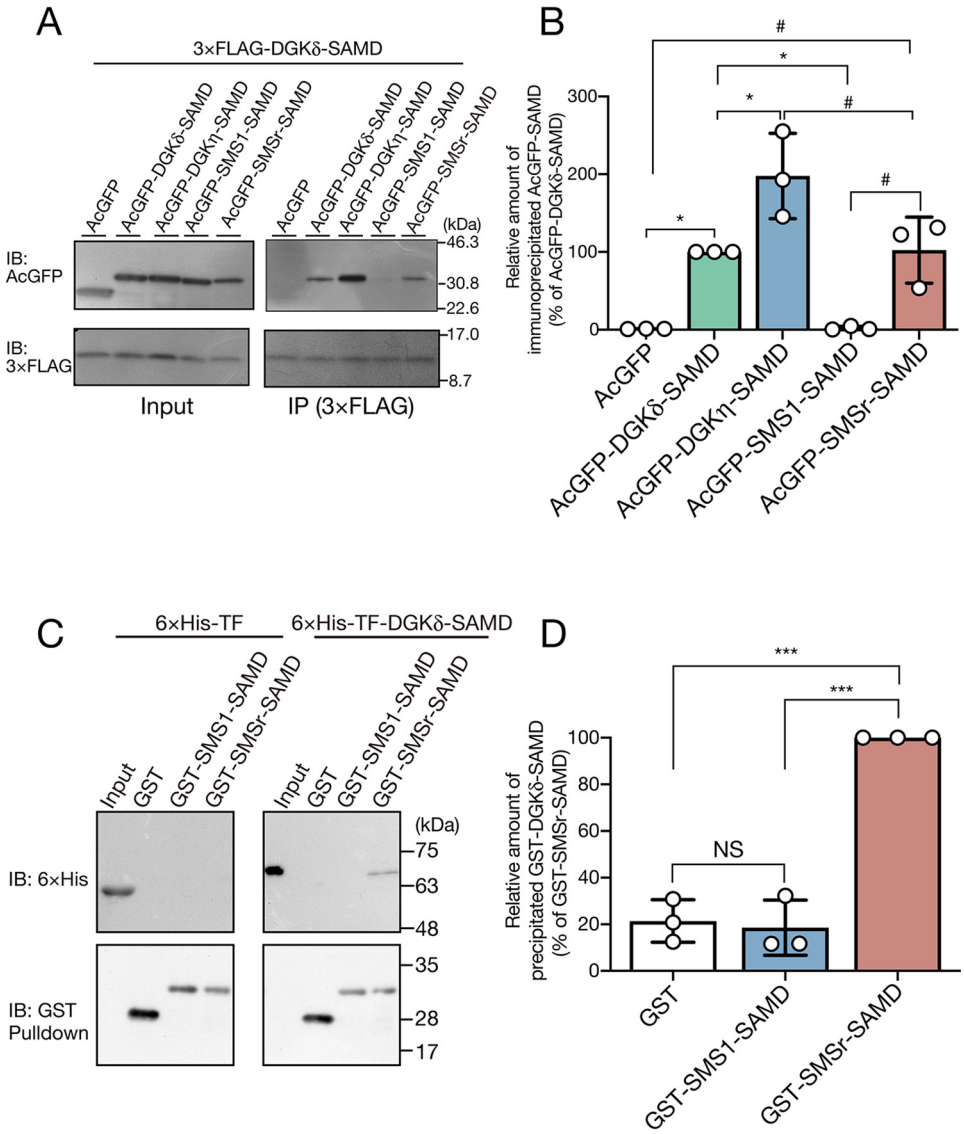

Figure 3. SMSr–SAMD directly interacts with DGKδ–SAMD. *A* and *B*, co-immunoprecipitation analysis of 3×FLAG–DGKδ–SAMD with AcGFP–DGKδ–SAMD, AcGFP–DGKη2–SAMD, AcGFP–SMS1–SAMD, or AcGFP–SMSr–SAMD. *A*, COS-7 cells were co-transfected with the following combinations of plasmids: 3×FLAG-tagged DGKδ–SAMD and either AcGFP alone, AcGFP–DGKδ–SAMD, AcGFP–DGKη2–SAMD, AcGFP–SMS1–SAMD, or AcGFP–SMSr–SAMD. At 24 h post-transfection, 5 μl of rabbit anti-DDDDK (FLAG)-tag antibody (PM020) was used for IP. Mouse monoclonal anti-FLAG antibody (F1804, 1:1000 dilution) and anti-GFP antibody (sc-9996, 1:1000 dilution) were used for immunoblotting (*IB*). A representative of three repeated experiments is shown. *Left panel*, cell lysate (*Input*); *right panel*, IP. *B*, densitometric quantification of AcGFP-fused proteins co-precipitated with 3×FLAG-tagged DGKδ–SAMD is represented as the ratio of the band intensities (% of AcGFP–DGKδ–SAMD). Band intensities were measured with densitometry using the Fiji software. The values are presented as the mean ± S.D. of three independent experiments. *, $p < 0.05$ *versus* DGKδ–SAMD; #, $p < 0.05$ *versus* SMSr–SAMD; and *NS*, not significant. *C* and *D*, pulldown assay of GST–SMS1–SAMD and GST–SMSr–SAMD with TF–DGKδ–SAMD. *C*, recombinant 6×His–TF-fused DGKδ–SAMD (20 μg) and either GST-fused SMS1–SAMD or SMSr–SAMD (20 μg) were used for the GST pulldown assays. GSH-Sepharose 4B beads were bound to either purified GST alone, GST–SMS1–SAMD, or GST–SMSr–SAMD. The proteins bound to beads were mixed and incubated for 1 h with either purified 6×His–TF alone or 6×His–TF–DGKδ–SAMD. The beads were washed four times, and proteins were eluted in 50 μl of 2 × SDS sample buffer. Anti-GST antibody (sc-138, 1:1000 dilution) and anti-6×His antibody (PM032, 1:1000 dilution) were used for immunoblotting (*IB*). A representative of three repeated experiments is shown. *Left panel*, 6×His–TF (vector alone); *right panel*, 6×His–TF–DGKδ–SAMD. *D*, band intensities were measured with densitometry using the Fiji software. The quantities of 6×His–TF–DGKδ–SAMD co-precipitated with GST–fusion proteins are represented as the ratio of the band intensities. GST–SMSr–SAMD was set to 100%. The values are presented as the mean ± S.D. of three independent experiments. ***, $p < 0.005$ *versus* GST–SMSr–SAMD, and *NS*, not significant.

To verify whether SMSr–SAMD interacted with DGKδ–SAMD directly or indirectly, we performed a GSH *S*-transferase (GST)-pulldown assay using purified GST-fused SMSr–SAMD or SMS1–SAMD and hexahistidine (6×His)-tagged trigger factor (TF)-fused DGKδ–SAMD (Fig. 1, *B* and *D*). When GST-tagged SMSr–SAMD was precipitated using GSH beads, 6×His–TF-tagged DGKδ–SAMD was co-sedimented (Fig. 3, *C* and *D*). However, 6×His–TF-DGKδ–SAMD was not co-sedimented with GST–SMS1–SAMD or GST alone. These results indicated that the DGKδ–SAMD directly interacted with the SMSr–SAMD.

SMSr interacted with DGKδ via SMSr–SAMD

Unfortunately, the appropriate antibodies to detect endogenous SMSr and to conduct its immunoprecipitation were unavailable. Thus, to verify whether full-length DGKδ2 and SMSr interacted with each other, 3×FLAG-tagged DGKδ2 and either V5-tagged SMS1, SMS2, or SMSr (Fig. 1) were co-ex-

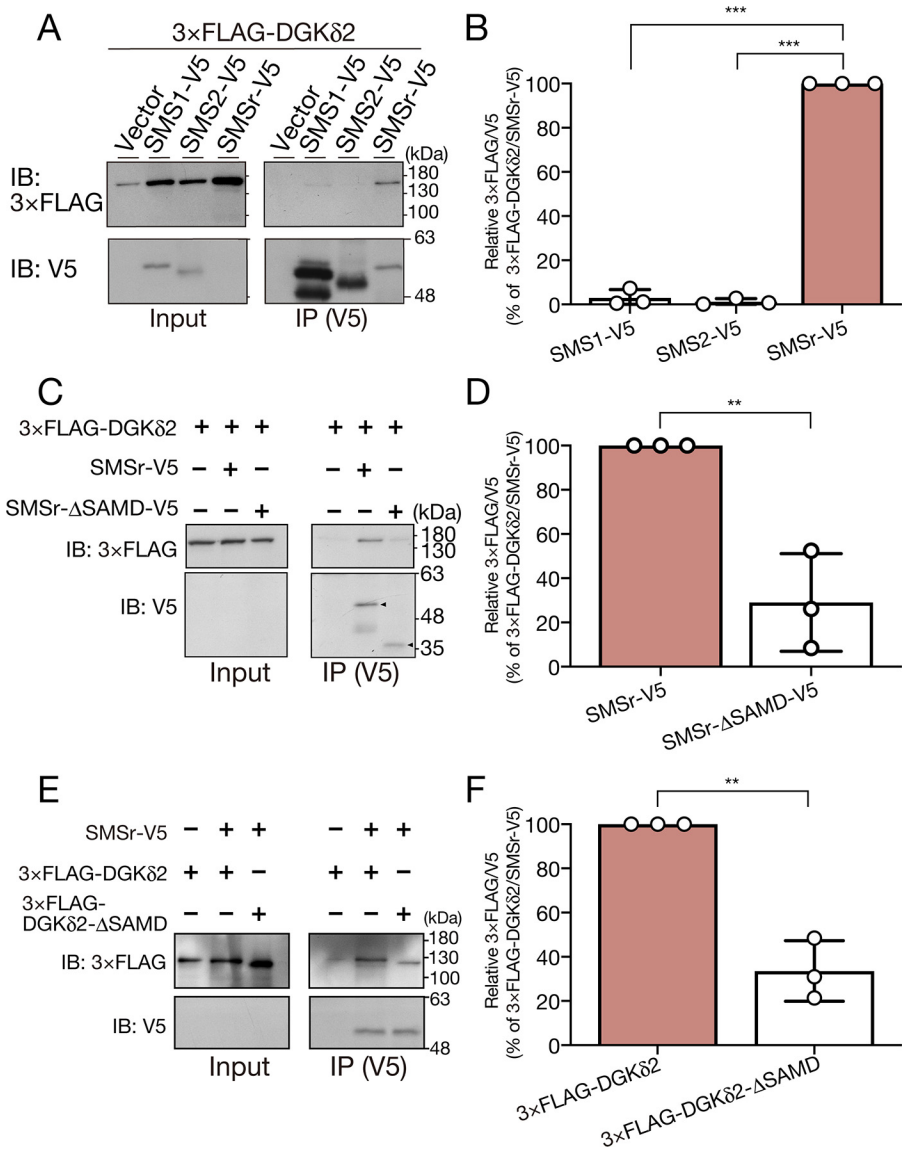

Figure 4. Hetero-oligomerization between DGKδ2 and SMSr through their SAMDs. *A* and *B*, hetero-oligomerization between DGKδ2 and SMSr. *A*, COS-7 cells were co-transfected with p3×FLAG-CMV-DGKδ2 and either pcDNA4/TO-SMS1–V5, pcDNA4/TO-SMS2–V5, or pcDNA4/TO-SMSr–V5. Anti-V5-tag antibody (1.5 μg, clone E10/V4RR) was used for IP. Anti-FLAG antibody (F1804, 1:1000 dilution) and anti-V5 antibody (clone E10/V4RR, 1:1000 dilution) were used for immunoblotting (*IB*). A representative of three repeated experiments is shown. *Left panel,* cell lysate (*Input*); *right panel*, *IP*. *B,* band intensities were measured with densitometry using the Fiji software. The densitometric quantification of 3×FLAG–DGKδ2 precipitated with V5-tagged proteins is represented as the ratio of the band intensities (% of 3×FLAG–DGKδ2 co-immunoprecipitated with SMSr–V5). The values are presented as the mean ± S.D. of three independent experiments. ***, $p < 0.005$ *versus* SMSr–V5. *C* and *D*, hetero-oligomerization between DGKδ2 and SMSr–ΔSAMD. *C*, COS-7 cells were co-transfected with p3×FLAG-CMV-DGKδ2 and either pcDNA4/TO-SMSr–V5 or pcDNA4/TO-SMSr–ΔSAMD. Anti-V5-tag antibody (1.5 μg) was used for IP. Anti-FLAG antibody and anti-V5 antibody were used for immunoblotting (*IB*). A representative of three repeated experiments is shown. *Left panel*, cell lysate (*Input*); *right panel*, *IP*. *D,* band intensities were measured with densitometry using the Fiji software. The densitometric quantification of 3×FLAG–DGKδ2 precipitated with V5-tagged proteins is represented as the ratio of the band intensities (% of DGKδ co-immunoprecipitated with SMSr–V5). The values are presented as the mean ± S.D. of three independent experiments. **, $p < 0.01$ *versus* SMSr–V5. *E* and *F,* hetero-oligomerization between DGKδ2–ΔSAMD and SMSr. *E*, COS-7 cells were co-transfected with pcDNA4/TO-SMSr–V5 and either p3×FLAG-CMV-DGKδ2 or p3×FLAG-CMV-DGKδ2-ΔSAMD. Anti-V5-tag antibody (1.5 μg) was used for IP. Anti-FLAG antibody and anti-V5 antibody were used for immunoblotting. A representative of three repeated experiments is shown. *Left panel*, cell lysate (*Input*); *right panel*, *IP*. *F*, band intensities were measured with densitometry using the Fiji software. The densitometric quantification of 3×FLAG–DGKδ2 precipitated with V5-tagged proteins is represented as the ratio of the band intensities (% of 3×FLAG–DGKδ co-immunoprecipitated with SMSr–V5). The values are presented as the mean ± S.D. of three independent experiments. **, $p < 0.01$ *versus* 3×FLAG–DGKδ2.

pressed in COS-7 cells, and the cell lysates were used for a co-immunoprecipitation analysis using anti-V5 antibody. We found that 3×FLAG–DGKδ2 was co-immunoprecipitated with SMSr–V5, but not with SMS1–V5, SMS2–V5, or V5 alone (Fig. 4, *A* and *B*), indicating that DGKδ2 associated with SMSr in cells.

We next examined the effect of the deletion of the SMSr–SAMD on the interaction between SMSr and DGKδ2 by co-immunoprecipitation analysis. We found that 3×FLAG–DGKδ2 and either V5-tagged full-length SMSr (SMSr–V5) or SAMD-deleted SMSr (SMSr–ΔSAMD–V5) (Fig. 1) were co-expressed in COS-7 cells. The V5-tagged proteins in cell lysates were immunoprecipitated with the anti-V5 antibody. Compared with full-length SMSr, the amount of DGKδ2 co-precipitated with the SMSr–ΔSAMD was significantly reduced (by about 75%) (Fig. 4, *C* and *D*). We also examined the effect of the

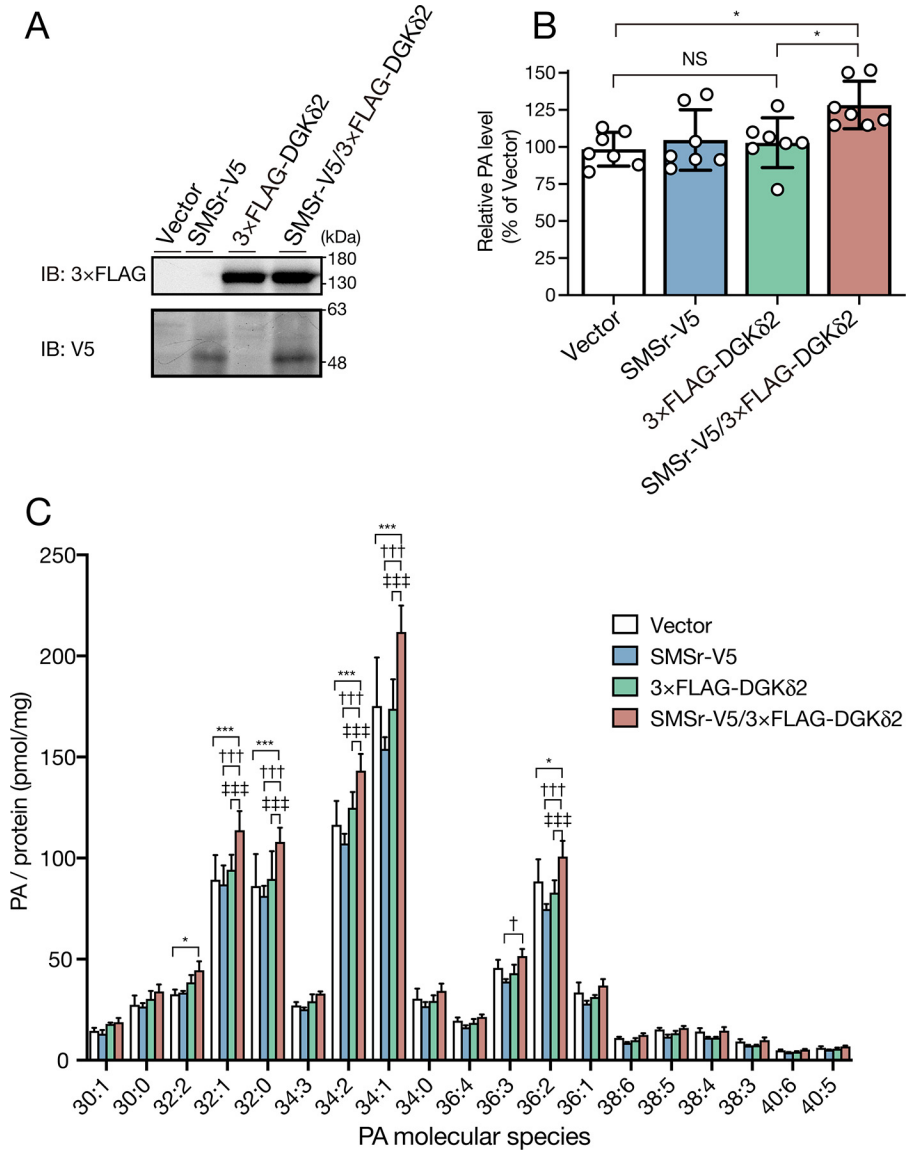

Figure 5. Changes in the amounts of total PA and PA molecular species in COS-7 cells by overexpressing SMSr and/or DGKδ2. *A–C*, COS-7 cells were co-transfected with the following four combinations of plasmids: either p3×FLAG–CMV vector alone or p3×FLAG-CMV-DGKδ2 and either pcDNAC4/TO vector alone or pcDNAC4/TO-SMSr–V5. After 24 h of transfection, cells were lysed in 900 μl of ice-cold PBS. Lysates (700 μl) were used for the quantitation of PA molecular species; 20 μl of lysates were used for immunoblotting (*IB*) to confirm the expression of 3×FLAG–DGKδ2; 150 μl of lysates were immunoprecipitated with anti-V5 antibody, followed by immunoblotting to confirm the expression of SMSr–V5, and 10 μl of lysates were used for the measurement of protein concentration. *A,* immunoblot analysis. Anti-FLAG antibody and anti-V5 antibody were used for immunoblotting. *B,* total PA levels in the COS-7 cells overexpressing 3×FLAG–DGKδ2 and/or SMSr–V5 were quantified using the LC-tandem MS (LC-MS/MS) method described under "Experimental procedures." The values are presented as the mean ± S.D. ($n = 7$). *, $p < 0.05$ *versus* the PA levels in cells overexpressing both 3×FLAG–DGKδ2 and SMSr–V5 (SMSr–V5/3×FLAG–DGKδ2), and *NS* is not significant. *C,* major PA molecular species were quantified using the LC-MS/MS method. The MS peaks are presented in the form of *X*:*Y*, where *X* is the total number of carbon atoms, and *Y* is the total number of double bonds in both acyl chains of the PA. The values are presented as the mean ± S.D. ($n = 4$). *, $p < 0.05$; ***, $p < 0.005$ (*Vector* alone *versus* SMSr–V5/3×FLAG–DGKδ2). †, $p < 0.05$; †††, $p < 0.005$ (SMSr–V5 *versus* SMSr–V5/3×FLAG–DGKδ2), and ‡‡‡, $p < 0.005$ (3×FLAG–DGKδ2 *versus* SMSr–V5/3×FLAG–DGKδ2).

deletion of the SAMD in DGKδ2 on the SMSr–DGKδ2 interaction using COS-7 cells overexpressing SMSr and either DGKδ2–ΔSAMD or DGKδ2 (Fig. 1, *B* and *D*). Similar to the SAMD deletion mutant of SMSr, DGKδ2–ΔSAMD showed a markedly weaker interaction than the interaction with DGKδ2 (Fig. 4, *E* and *F*). Taken together, these results indicated that DGKδ2 interacted with SMSr via their SAMDs.

SMSr enhanced 16:0- and/or 16:1-containing PA species' production of DGKδ2 in COS-7 cells

To address the functional relationship between SMSr and DGKδ2, we analyzed changes in the amounts of PA in COS-7 cells overexpressing 3×FLAG–DGKδ2 and/or SMSr–V5 (Fig. 5). Compared with COS-7 cells transfected with vector alone, total PA levels were not substantially changed in the cells overexpressing DGKδ2 or SMSr alone. However, total PA levels in COS-7 cells overexpressing both DGKδ2 and SMSr were significantly increased by ~20% (Fig. 5*B*). In particular, the levels of 32:2-PA (a 40% increase compared with control cells), 32:1-PA (a 28% increase), 32:0-PA (a 25% increase), 34:2-PA (a 23% increase), and 34:1-PA (a 21% increase) in COS-7 cells expressing both SMSr and DGKδ2 were significantly increased more than 20% compared with those in control cells (Fig. 5*C*).

Table 1
Identification of the acyl species in each PA molecular species in COS-7 cells

PA molecular species	Identified acyl chains[a]			
30:1	12:0/18:1 (6.0%)	14:0/16:1 (55.8%)	14:1/16:0 (38.1%)	
30:0	14:0/16:0 (100.0%)			
32:3	14:0/18:3 (23.8%)	14:1/18:2 (49.2%)	16:1/16:2 (26.9%)	
32:2	14:0/18:2 (6.1%)	14:1/18:1 (10.8%)	16:0/16:2 (2.3%)	16:1/16:1 (80.8%)
32:1	10:0/22:1 (0.8%)	14:0/18:1 (14.9%)	14:1/18:0 (0.8%)	16:0/16:1 (83.5%)
32:0	10:0/22:0 (0.4%)	14:0/18:0 (1.0%)	16:0/16:0 (98.6%)	
34:3	16:0/18:3 (21.5%)	16:1/18:2 (73.8%)	16:2/18:1 (4.7%)	
34:2	14:0/20:2 (10.3%)	16:0/18:2 (33.1%)	16:1/18:1 (56.6%)	
34:1	10:0/24:1 (0.7%)	14:0/20:1 (5.8%)	16:0/18:1 (89.4%)	16:1/18:0 (4.1%)
34:0	14:0/20:0 (2.1%)	16:0/18:0 (97.9%)		
36:4	16:0/20:4 (49.9%)	16:1/20:3 (7.0%)	18:1/18:3 (16.2%)	18:2/18:2 (27.0%)
36:3	16:0/20:3 (9.4%)	18:0/18:3 (2.8%)	18:1/18:2 (87.7%)	
36:2	14:0/22:2 (1.0%)	16:0/20:2 (1.9%)	18:0/18:2 (13.2%)	18:1/18:1 (83.9%)
36:1	14:0/22:1 (9.0%)	16:0/20:1 (8.1%)	18:0/18:1 (82.9%)	
38:6	16:0/22:6 (83.4%)	16:1/22:5 (8.2%)	18:1/20:5 (8.4%)	
38:5	16:0/22:5 (38.4%)	18:0/20:5 (9.0%)	18:1/20:4 (52.6%)	
38:4	16:1/22:3 (8.7%)	18:0/20:4 (70.7%)	18:1/20:3 (20.6%)	
38:3	16:0/22:3 (23.8%)	16:1/22:2 (34.6%)	18:0/20:3 (41.6%)	
40:6	16:0/24:6 (20.7%)	16:1/24:5 (12.4%)	18:0/22:6 (40.2%)	18:1/22:5 (26.6%)
40:5	16:0/24:5 (52.2%)	16:1/24:4 (14.8%)	18:0/22:5 (32.9%)	

[a] The relative abundance (%) was based on the peak areas of the fragment ions (ESI-MS/MS) for each molecular ion.

LC-MS/MS analysis showed that the primary fatty acids bound to these PA species were as follows: 32:2 consisted of 16:1/16:1 (80.8%); 32:1 consisted of 16:0/16:1 (83.5%); 32:0 consisted of 16:0/16:0 (98.6%); 34:2 consisted of 16:1/18:1 (56.6%) and 16:0/18:2 (33.1%); and 34:1 consisted of 16:0/18:1 (89.4%) (Table 1). These results strongly suggested that SMSr augmented PA generation from DGKδ2, which primarily produces 16:0- and/or 16:1-containing PA molecular species (15), in cells. It is also possible that DGKδ2 and SMSr are functionally linked and that SMSr acts in an upstream pathway of DGKδ2.

SMSr produced 16:0- and/or 16:1-containing DG species in COS-7 cells

To support the possibility that SMSr provided DG to DGKδ2, we next tested whether SMSr produced 16:0- or 16:1-containing DG molecular species, which are preferably phosphorylated by DGKδ2 (Fig. 5 and Table 1) (15), by measuring DG levels in SMSr-overexpressing cells (Fig. 6*A*). Compared with control cells, total DG levels in SMSr-overexpressing cells were significantly increased by ~14% (Fig. 6*B*). In particular, 16:0- and/or 16:1-containing DG species, such as 14:0/16:1 (30:1)-DG (a 42% increase), 14:0/16:0 (30:0)-DG (a 34% increase), 16:1/16:1 (32:2)-DG (a 45% increase), 16:0/16:1 (32:1)-DG (a 24% increase), 16:1/18:2 (34:3)-DG (a 28% increase), and 16:0/18:2-DG (a 20% increase), were significantly increased more than 20% (Fig. 6*C* and Table 2). Therefore, it was possible that SMSr provided 16:0- and/or 16:1-containing DG species to DGKδ2 and that, subsequently, DGKδ2 phosphorylated the DG species generated by SMSr.

DGKδ2 enzyme activity was increased by SMSr through their SAMDs in vitro

We next examined whether DGKδ2 activity was enhanced by complex formation with SMSr via their SAMDs. First, 6×His-tagged SMSr, SMSr–ΔSAMD, and DGKδ2 (Fig. 1, *B* and *D*) were expressed using COS-7 cells and purified by Ni-affinity chromatography (Fig. 7*A*). We tested whether the activity of 6×His-tagged DGKδ2 was enhanced by SMSr *in vitro* in the presence of DG (in the absence of PE and ceramide). Interestingly, when adding purified SMSr to purified DGKδ2 (stoichiometry, ~3:1), DGK activity was significantly increased (Fig. 7*B*). However, when adding SMSr–ΔSAMD to DGKδ2, DGK activity was not significantly increased (Fig. 7*C*), suggesting that SMSr activated DGKδ2 in a SAMD-dependent manner. To test whether SMSr–SAMD alone enhanced DGKδ2 activity, we added GST–SMSr–SAMD (Fig. 1*D*), which was expressed in *Escherichia coli* and purified by GSH-affinity chromatography, to purified DGKδ2. The activity of DGKδ2 was significantly increased by the addition of the GST–SMSr–SAMD (Fig. 7*D*). These results strongly suggested that, in addition to DG supply, SMSr directly enhanced DGKδ2 activity via the SMSr–SAMD.

The results of Fig. 7*D* implied that the disturbance of homodimerization of DGKδ2 by SMSr–SAMD enhanced its activity. To verify this, DGKδ1, DGKδ2, and their SAMD deletion mutants were expressed in COS-7 cells, and DGK activities in cell lysates were measured using a luminescence-based (ADP-glo) kinase assay (Fig. 8) (26). The DGK activities of SAMD deletion mutants of DGKδ (both isoform 1 and 2) were significantly increased compared with their WT enzymes (Fig. 8*B*). These results suggested that the SAMD suppressed the activity of DGKδ and that the SMSr–SAMD increased DGKδ2 activity by disrupting its homo-oligomers.

Discussion

A DG-providing pathway for DGKδ, which would play an important role in type 2 diabetes pathogenesis, has been unclear. In this study, we, for the first time, demonstrate that DGKδ2 was associated with SMSr, a DG-generating enzyme, via their SAMDs (Figs. 3 and 4). Moreover, the overexpression of SMSr significantly enhanced the production of PA in COS-7 cells overexpressing DGKδ (Fig. 5). Thus, these data suggested the possibility that SMSr acts as a DG-providing enzyme upstream of DGKδ2 (Fig. 9). Therefore, it is likely that these enzymes compose a new pathway independent of phosphatidylinositol turnover.

We demonstrated that DGKδ–SAMD directly interacted with SMSr–SAMD (Figs. 3 and 9*A*). Moreover, we showed that full-length DGKδ2 and SMSr associated with each other and

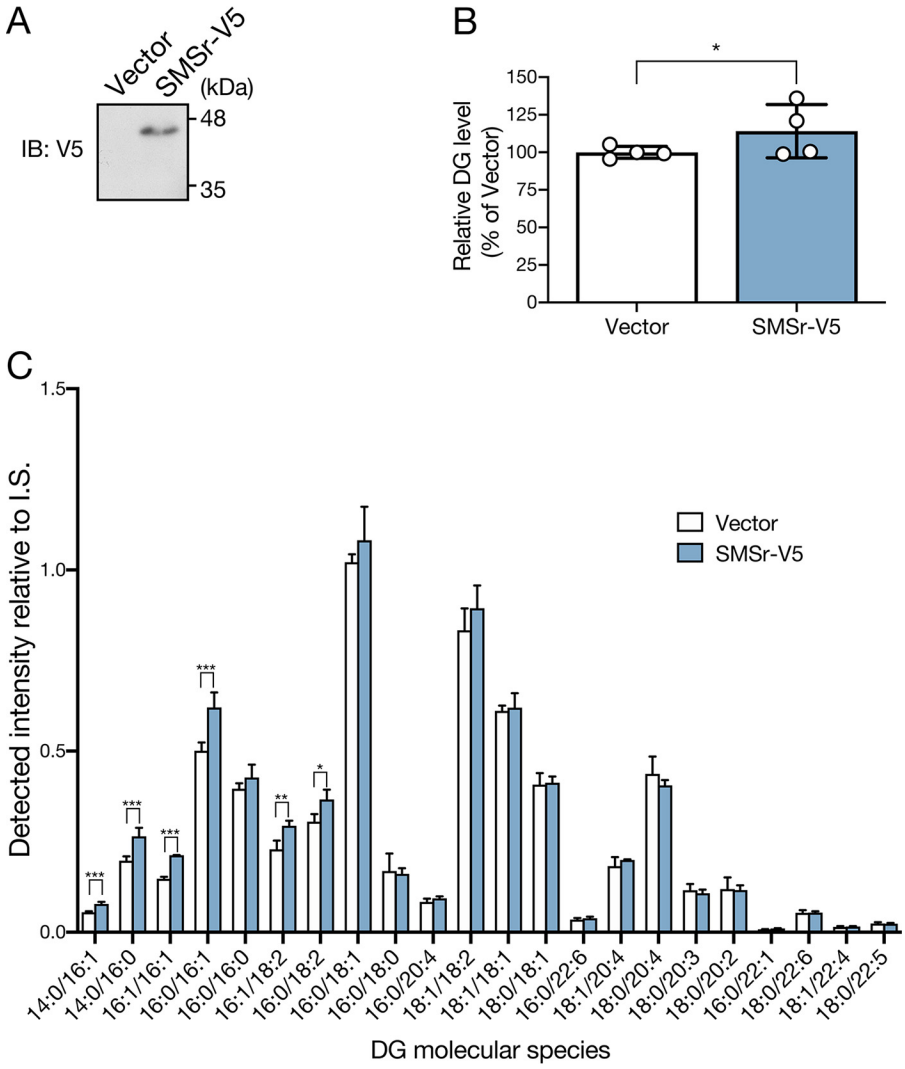

Figure 6. Changes in the amounts of total DG and DG molecular species in COS-7 cells by overexpressing SMSr. *A* and *B*, COS-7 cells were transfected with pcDNAC4/TO vector alone or pcDNAC4/TO-SMSr–V5. After 24 h of transfection, cells were lysed in 900 μl of ice-cold PBS. *A*, lysates (150 μl) were immunoprecipitated with an anti-V5 antibody, followed by immunoblotting to confirm the expression of SMSr–V5 using the anti-V5 antibody. *B*, total DG levels in COS-7 cells transfected with vector alone or pcDNAC4/TO-SMSr–V5 were measured using the LC-MS/MS. The values are presented as the mean ± S.D. ($n = 4$). *, $p < 0.05$. *C*, major DG molecular species were quantified using LC-MS/MS method. The MS peaks are presented in the form of *X:Y*, where *X* is the total number of carbon atoms, and *Y* is the total number of double bonds in both acyl chains of the DG. The DG molecular species in the sample were quantified using internal standard (*I.S.*). The values are presented as the mean ± S.D. ($n = 4$). *, $p < 0.05$; **, $p < 0.01$; and ***, $p < 0.005$.

Table 2
Identification of the acyl species in each DG molecular species in COS-7 cells

DG molecular species	Identified acyl chains[a]					
30:1	10:0/20:1 (1.1%)	12:0/18:1 (6.5%)	14:0/16:1 (68.3%)	14:1/16:0 (24.1%)		
30:0	10:0/20:0 (1.4%)	12:0/18:0 (1.7%)	14:0/16:0 (96.9%)			
32:2	14:0/18:2 (11.5%)	14:1/18:1 (4.2%)	16:0/16:2 (2.9%)	16:1/16:1 (81.3%)		
32:1	14:0/18:1 (24.0%)	16:0/16:1 (76.0%)				
32:0	12:0/20:0 (1.1%)	14:0/18:0 (1.7%)	16:0/16:0 (97.2%)			
34:3	16:0/18:3 (6.3%)	16:1/18:2 (91.5%)	16:2/18:1 (2.2%)			
34:2	16:0/18:2 (31.1%)	16:1/18:1 (68.9%)				
34:1	16:0/18:1 (93.1%)	16:1/18:0 (6.9%)				
34:0	14:0/20:0 (1.3%)	16:0/18:0 (98.7%)				
36:4	16:0/20:4 (22.5%)	16:1/20:3 (3.1%)	18:1/18:3 (14.4%)	18:2/18:2 (60.0%)		
36:3	16:0/20:3 (4.7%)	16:1/20:2 (1.4%)	18:0/18:3 (1.8%)	18:1/18:2 (92.2%)		
36:2	16:0/20:2 (2.6%)	16:1/20:1 (1.0%)	18:0/18:2 (19.6%)	18:1/18:1 (76.8%)		
36:1	14:0/22:1 (0.9%)	16:0/20:1 (17.1%)	16:1/20:0 (0.9%)	18:0/18:1 (81.1%)		
38:6	14:0/24:6 (3.3%)	16:0/22:6 (27.3%)	16:1/22:5 (8.1%)	18:1/20:5 (19.6%)	18:2/20:4 (40.1%)	18:3/20:3 (1.6%)
38:5	14:0/24:5 (1.7%)	16:0/22:5 (11.2%)	18:0/20:5 (6.7%)	18:1/20:4 (74.0%)	18:2/20:3 (6.5%)	
38:4	14:0/24:4 (1.1%)	16:0/22:4 (2.6%)	18:0/20:4 (93.1%)	18:2/20:2 (3.2%)		
38:3	16:0/22:3 (1.8%)	18:0/20:3 (72.2%)	18:1/20:2 (20.6%)	18:2/20:1 (5.4%)		
40:6	16:0/24:6 (7.4%)	16:1/24:5 (6.2%)	18:0/22:6 (59.6%)	18:1/22:5 (22.5%)	18:2/22:4 (1.8%)	20:2/20:4 (2.5%)
40:5	16:0/24:5 (33.1%)	16:1/24:4 (2.1%)	18:0/22:5 (40.3%)	18:1/22:4 (14.9%)	18:2/22:3 (1.3%)	20:1/20:4 (8.3%)

[a] The relative abundance (%) was based on the peak areas of the fragment ions (ESI-MS/MS) for each molecular ion.

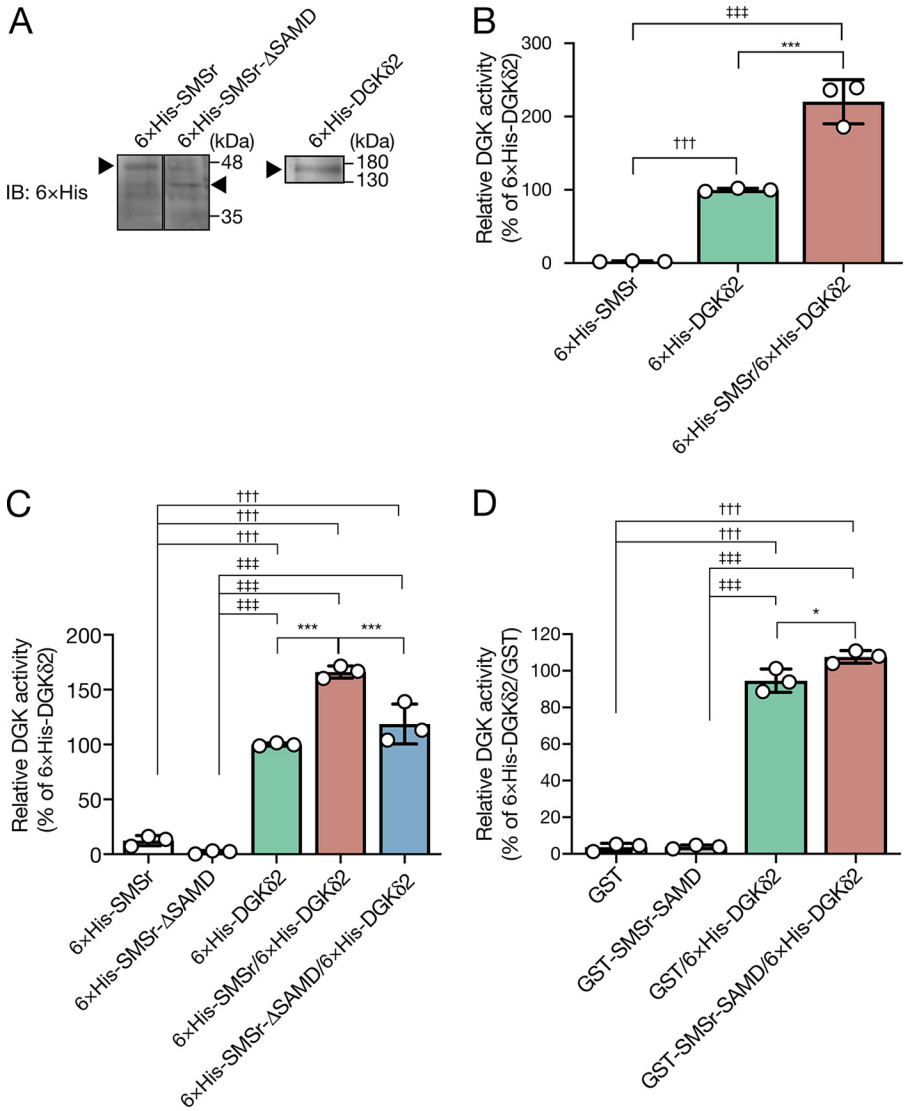

Figure 7. SMSr enhances DGKδ2 activity *in vitro* via their SAMDs. *A,* purification of 6×His–SMSr, 6×His–SMSr–ΔSAMD, and 6×His–DGKδ2 expressed in COS-7 cells using affinity chromatography on a Ni-Sepharose 6 Fast Flow column. Purified 6×His–SMSr, 6×His–SMSr–ΔSAMD, and 6×His–DGKδ2 were detected by immunoblot using anti-6×His antibody. *B,* effects of SMSr on DGKδ2 activity *in vitro* in the presence of DG. The activities of DGKδ2 were measured using LC-MS/MS. The values are presented as the mean ± S.D. ($n = 3$). ***, $p < 0.05$ (DGKδ2 *versus* SMSr/DGKδ2); †††, $p < 0.005$ (SMSr *versus* SMSr/DGKδ2); ‡‡‡, $p < 0.005$ (DGKδ2 *versus* SMSr). *C,* effects of SMSr, SMSr–ΔSAMD, and SMSr–SAMD on the activity of DGKδ2 *in vitro* in the presence of DG. The activities of DGKδ2 were measured using LC-MS/MS. The values are presented as the mean ± S.D. ($n = 3$). ***, $p < 0.005$ (SMSr/DGKδ2 *versus* other DGKδ2-containing samples (6×His–DGKδ2 alone or 6×His–DGKδ2/6×His–SMSr–ΔSAMD)); †††, $p < 0.005$ (6×His–SMSr *versus* 6×His–DGKδ2-containing samples); ‡‡‡, $p < 0.005$ (6×His–SMSr–ΔSAMD *versus* 6×His–DGKδ2-containing samples). *D,* effect of SMSr–SAMD alone on DGKδ2 activity *in vitro* in the presence of DG. GST–SMSr–SAMD and GST alone were expressed in *E. coli* and purified. The values are presented as the mean ± S.D. ($n = 3$). *, $p < 0.05$ (GST–SMSr–SAMD/6×His–DGKδ2 *versus* GST/6×His–DGKδ2); †††, $p < 0.005$ (GST *versus* 6×His–DGKδ2-containing samples), and ‡‡‡, $p < 0.005$ (GST–SMSr–SAMD *versus* 6×His–DGKδ2-containing samples).

that their SAMDs mainly contributed to the association (Fig. 4). SAMD, which is an evolutionally conserved protein–protein interaction domain, is known to occur in a wide range of proteins (more than 200) (27). SAMDs generally form homodimers between the same proteins and between closely-related family proteins. However, in some cases, a heterodimer between completely different proteins, such as between Connector enhancer of KSR (kinase suppressor of Ras)–SAMD and Hyphen–SAMD (28) and between Src homology 2 domain-containing phosphoinositide-5-phosphatase 2–SAMD and Ephrin A2 receptor–SAMD are formed (29). In this study, we identified a new combination of heterodimers between completely different proteins, DGKδ and SMSr, through their SAMDs.

Five and four (Asp-1183, Val-1192, Gly-1193, and Lys-1196) of five key residues (Glu-1175, Asp-1183, Val-1192, Gly-1193, and Lys-1196 in DGKδ2) involved in DGKδ–SAMD homodimerization are conserved in DGKη2–SAMD and SMSr–SAMD, respectively, but are not in the SMS1–SAMD (Fig. 2) (22). Moreover, immunoprecipitation and pulldown analyses showed that DGKδ–SAMD could form a heterodimer with the DGKη2–SAMD and SMSr–SAMD, whereas DGKδ–SAMD was not able to interact with the SMS1–SAMD (Fig. 3). These results implied that the four (Asp-1183, Val-1192, Gly-1193, and Lys-1196) key residues involved in the formation of the DGKδ–SAMD homodimer were important for heteromeric dimerization. To verify whether these four residues in the

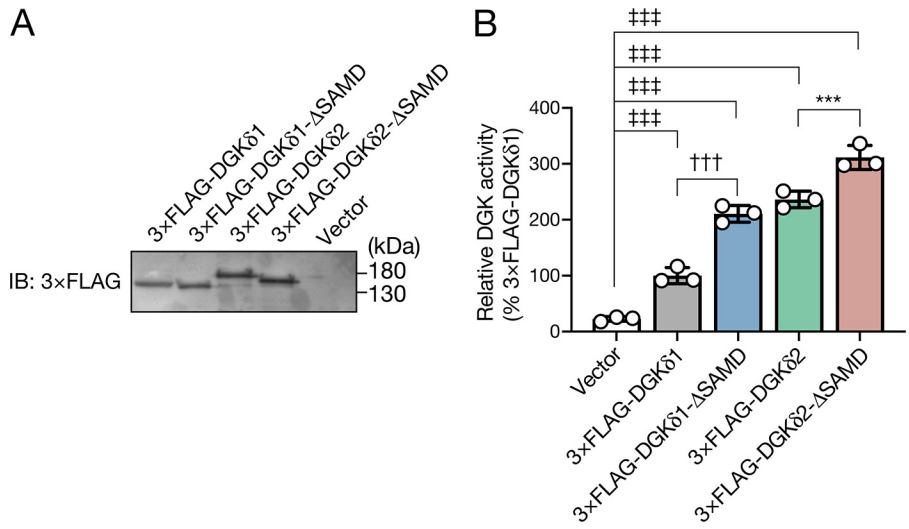

Figure 8. Effect of SAMD deletion on DGKδ activity. *A,* COS-7 cells were transfected with plasmids encoding either 3×FLAG–DGKδ1, 3×FLAG–DGKδ2, 3×FLAG–DGKδ1–ΔSAMD, or 3×FLAG–DGKδ2–ΔSAMD. *B,* cell lysates (15 μg of protein/sample) were assayed for DGK activity using the ADP-Glo kinase assay kit. To facilitate the comparison, background activities (the control cells transfected with the vector alone) were subtracted and then the values were normalized for protein expression levels assessed by immunoblot (*IB*). The activity of 3×FLAG–DGKδ1 was set to 100%. The values are presented as the mean ± S.D. ($n = 3$). ***, $p < 0.005$ (3×FLAG–DGKδ2 *versus* 3×FLAG–DGKδ2–ΔSAMD); †††, $p < 0.005$ (3×FLAG–DGKδ1 *versus* 3×FLAG–DGKδ1–ΔSAMD), and ‡‡‡, $p < 0.005$ (Vector *versus* other samples).

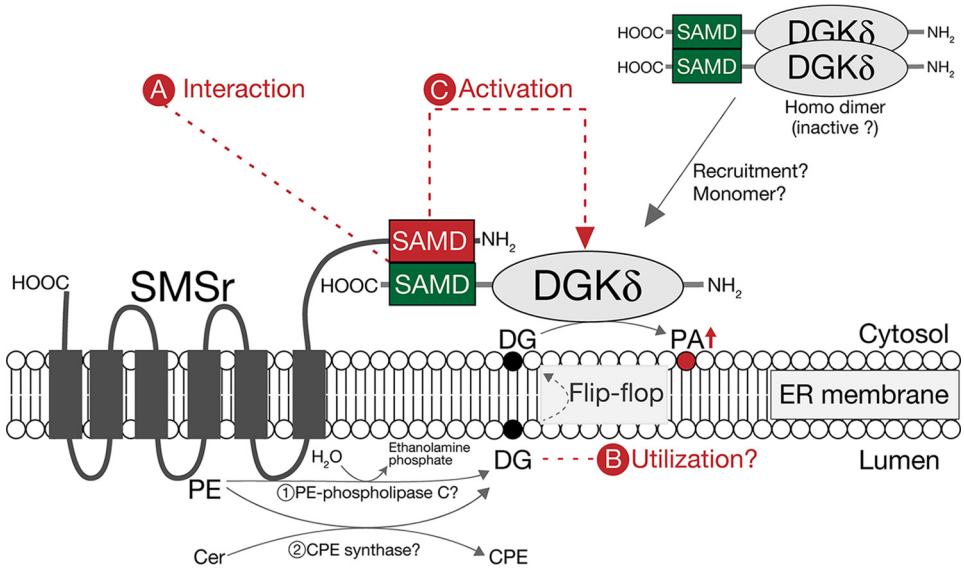

Figure 9. Model for a new DG metabolism pathway involving SMSr and DGKδ. In this study, we demonstrated that DGKδ–SAMD directly interacts with SMSr–SAMD (*A*). It is possible that SMSr acts upstream of DGKδ and supplies DG to the enzyme. There is the possibility that SMSr possesses not only ceramide phosphoethanolamine (*CPE*) synthase activity but also PE-specific phospholipase C activity.[3] *B,* SMSr–SAMD may disrupt the homodimerization of DGKδ2, which attenuates its DGK activity and, consequently, enhances DGKδ2 activity (*C*). Alternatively, SMSr, which is a transmembrane protein, may recruit DGKδ2 to the DG-containing membrane via their SAMDs (*C*). *Cer*, ceramide; PE; phosphatidylethanolamine; SMSr, sphingomyelin synthase-related protein.

DGKδ–SAMD were critical for forming a heteromeric complex with the SMSr–SAMD, we prepared single-point mutants of the DGKδ–SAMD/D1183G, V1192E, G1193D, and K1196E. Co-immunoprecipitation analysis showed that the co-sedimented level of only the DGKδ–SAMD-G1193D mutant tended to be decreased, but there was no significant difference.[3] This result suggested that Gly-1193 was one of the key residues for the DGKδ–SAMD/SMSr–SAMD heteromeric complex. However, it was possible that other residues were also important for the heterodimerization.

To determine the functional relationship between DGKδ and SMSr, we investigated changes in the amounts of PA molecular species in COS-7 cells overexpressing DGKδ and/or SMSr using LC-MS/MS (Fig. 5). We found that the overexpression of SMSr significantly (more than 20%) enhanced the production of palmitic acid (16:0)- and/or palmitoleic acid (16:1)-containing PA species, such as 30:0 (14:0/16:0)-PA, 32:1 (16:0/16:1)-PA, 32:0 (16:0/16:0)-PA, 34:1 (16:0/18:1)-PA, and 34:2 (16:1/18:1 and 16:0/18:2)-PA in COS-7 cells overexpressing DGKδ (Fig. 5 and Table 1). Therefore, it was possible that SMSr acted upstream of DGKδ and supplied DG to the enzyme (Fig. 9*B*). Moreover, several lines of evidence supported this hypothesis.

[3] C. Murakami and F. Sakane, unpublished work.

First, the fatty acid compositions of PA species produced by DGKδ (Fig. 5 and Table 1) were similar to those produced under physiological conditions. We previously revealed that the suppression of DGKδ2 expression decreased high-glucose–induced production of 16:0- and/or 16:1-containing PA species, such as 30:0 (14:0/16:0)-PA, 30:1 (14:0/16:1)-PA, 32:1 (16:0/16:1)-PA, 32:0 (16:0/16:0)-PA, 34:1 (16:0/18:1)-PA, and 34:0 (16:0/18:0)-PA, in C2C12 myoblast cells (15).

Second, the fatty acid compositions of DG species produced by SMSr were similar to those of PA species produced by DGKδ. Overexpression of SMSr in COS-7 cells increased the amount of DG, especially 16:0- and/or 16:1-containing DG molecular species, such as 30:1 (14:0/16:1)-DG, 30:0 (14:0/16:0)-DG, 32:2 (16:1/16:1)-DG, 32:1 (16:0/16:1)-DG, 34:3 (16:1/18:2)-DG, and 34:2 (16:0/18:2)-DG (Fig. 6 and Table 2).

Third, both SMSr–SAMD and DGKδ2 (DGKδ2–SAMD) exist in the cytoplasm and are able to associate with each other as shown in Fig. 9. Topological analysis using the *N*-glycosylation gel-shift assay showed that the N-terminal SAMD is cytosolic (30). DGKδ2 is also cytosolic (21, 31). Therefore, it was possible that the DGKδ2–SAMD interacted with SMSr via the SMSr–SAMD in the cytoplasm. In addition, DG is known to quickly diffuse across the lipid bilayer by the flip-flop mechanism (32, 33). Therefore, it is likely that the DG produced by SMSr immediately transverses the ER membrane from the lumen side to the cytosol leaflet and, consequently, is provided to DGKδ, as illustrated in Fig. 9*B*.

Fourth, SMSr and DGKδ2 were distributed in the same cells and tissues. DGKδ is highly expressed in skeletal muscle (31), and SMSr is also reported to be abundantly expressed in skeletal muscle (34). It was revealed that the mRNA level of SMSr was markedly higher than DGKδ in skeletal muscle– derived C2C12 myoblast cells.[3] Taken together, it is possible that endogenous DGKδ2 is able to interact with SMSr in skeletal muscles and myoblast cells. In addition to skeletal muscle, DGKδ was reported to be broadly expressed in multiple mouse tissues, in particular, and to be highly expressed in the brain and testis (35). Moreover, it was reported that SMSr is also widely expressed, with the highest expression in testis, brain, kidney, and pancreas (34). Thus, the expression pattern of DGKδ2 is similar to that of SMSr, suggesting that DGKδ2 and SMSr act in the same cells and tissues. Overall, these results allow us to speculate that DGKδ2 functionally links with SMSr, which acts upstream of DGKδ2 as a DG-supply enzyme. However, further studies are needed to clarify the linkage in more detail.

SMSr is known to show only weak ceramide phosphoethanolamine synthase activity (24). Interestingly, we unexpectedly found that purified SMSr generated DG even in the absence of ceramide when glycerophospholipid, such as PE or phosphatidylcholine (PC) alone, was added as a substrate.[3] Therefore, it is possible that, in addition to ceramide phosphoethanolamine synthase, SMSr is able to act as a PE- and PC-phospholipase C (PLC) to produce DG. It is interesting to further verify this possibility. We previously reported the possibility that D609 –sensitive enzymes, SMS and PC-PLC, are candidates for the DG-supply enzyme to DGKδ (15). Thus, it is noteworthy that D609 partly (~50%) inhibited the PLC activity of SMSr.[3]

The results of Fig. 7 suggested that SMSr activated DGKδ2 in a SAMD-dependent manner. We previously reported that DGKη2–SAMDs formed homodimers and suppressed the catalytic activity of DGKη2 (19). We confirmed that the DGKδ–SAMD also inhibited the catalytic activity of DGKδ2 by homodimerization (Fig. 8). Therefore, it was possible that SMSr–SAMD disrupted the homodimerization of DGKδ2, which attenuated its DGK activity and, consequently, enhanced the DGKδ2 activity (Fig. 9*C*). Alternatively, SMSr, which is a transmembrane protein, may recruit DGKδ2 to DG-containing micelles via their SAMDs (Fig. 9*C*).

In summary, this study, for the first time, showed that DGKδ2 and SMSr formed a heteromeric complex via their SAMDs. Moreover, the SAMD of SMSr activated DGKδ2. These results allow us to propose the alternative DG metabolic pathway "PE → SMSr → DG → DGKδ2 → PA" (Fig. 9). This pathway metabolized palmitic acid (16:0) and/or palmitoleic acid (16:1)-containing glycerolipids, but it did not utilize arachidonic acid (20:4)-containing glycerolipids derived from PI turnover. Therefore, it is likely that this new pathway is independent of PI turnover, although the substrate of DGK is generally thought to be derived from the PI-dependent pathway. The decrease of DGKδ protein and DG accumulation is known to regulate the pathogenesis of type 2 diabetes (14). Future studies exploring the mechanism by which SMSr-dependent DG supply and the linkage between SMSr and DGKδ are regulated will provide further insights into how type 2 diabetes is exacerbated.

Experimental procedures

Materials

Lipids—1,2-Dimyristoyl-*sn*-glycero-3-phosphate (14:0/14:0-PA) (catalog no. 830845) and 1-palmitoyl-2-oleoyl-*sn*-glycerol (16:0/18:1-DG) (catalog no. 800815) were obtained from Avanti Polar Lipids (Alabaster, AL). 1,2-Dimyristoyl-*sn*-glycerol (14:0/14:0-DG) (item no. 15077) and *N*-stearoyl-D-erythro-sphingosine (d18:1/18:0-Cer) (item no. 19556) were obtained from Cayman Chemical Co. (Ann Arbor, MI).

Antibodies—Rabbit polyclonal anti-His-tag antibody (PM032) and anti-DDDDK (FLAG)-tag antibody (PM020) were obtained from Medical and Biological Laboratories (Nagoya, Japan). Mouse monoclonal anti-V5 antibody (clone E10/V4RR, catalog no. MA5-15253) and Alexa Fluor 594–conjugated goat anti-mouse IgG (A-11005) were obtained from Thermo Fisher Scientific (Waltham, MA). Mouse monoclonal anti-FLAG–tag antibody (F1804) was purchased from Sigma. Mouse monoclonal anti-GFP antibody (sc-9996) and anti-GST antibody (sc-138) were obtained from Santa Cruz Biotechnology (Santa Cruz, CA). A peroxidase-conjugated goat anti-mouse IgG antibody was purchased from Bethyl Laboratories (Montgomery, TX). A peroxidase-conjugated goat anti-rabbit IgG antibody (11-036-045) was obtained from Jackson ImmunoResearch (West Grove, PA). We also used rabbit polyclonal anti-DGKδ antibody (WB-1), which was prepared previously (31).

Mice

C57BL/6N mice were obtained from SLC Japan, Inc. (Shizuoka, Japan). Tissues were removed immediately after decapitation. All procedures using C57BL/6N mice were conducted in compliance with the National Institutes of Health: Guide for the Care and Use of Laboratory Animals and the Institutional Animal Care and Use Committee of the University of Chiba approved the protocol (permission number: 29-195).

Reverse transcriptase-PCR

Total RNA was isolated from mouse testis using QIAzol Lysis Reagent (Qiagen, Venlo, Netherlands) and Direct-zol™ RNA Miniprep (Zymo Research, Irvine, CA) according to the protocol from the manufacturer. The cDNA was generated using transcriptor reverse transcriptase (Roche Diagnostics, Mannheim, Germany), as described previously (36).

Plasmids

We used the following nomenclature for epitope-tagged proteins: TagX-(protein) and (protein)-TagY means that TagX and TagY are located in the N and C termini of the protein, respectively. The expression vectors for human full-length SMS1, SMS2, and SMSr (SMS1–V5, SMS2–V5, and SMSr–V5), SAMD-deletion mutants of SMS1 (amino acid residues 69–413, henceforth referred to as SMS1–ΔSAMD–V5), and SMSr (amino acid residues 69–415, SMSr–ΔSAMD–V5) were generated by PCR using specific primers containing sequences corresponding to the V5 tag in front of the stop codon as described (Fig. 1*C*) (37–39). The resulting DNA sequences were verified to be correct by DNA sequencing. PCR products were subcloned into the pcDNA4TO plasmid (Invitrogen).

The cDNAs encoding human DGKδ2 and human DGKδ2–ΔSAMD that were subcloned into the expression plasmids, p3×FLAG-CMV (Sigma, Tokyo, Japan) and pAcGFP-C1 (Clontech-Takara Bio, Kusatsu, Japan), for expression in mammalian cells were generated as described (Fig. 1*B*) (21, 40–42). To express 6×His-tagged protein, human DGKδ, human SMSr, and SMSr–ΔSAMD (amino acid residues 79–413) were subcloned into the pSF-CMV-NH_2-His-EKT3 vector (OG332, Oxford Genetics, Begbroke, UK).

For bacterial expression, cDNAs encoding mouse SMS1–SAMD (amino acid residues 10–74), mouse SMSr–SAMD (amino acid residues 75–140), human DGKδ2–SAMD (amino acid residues 1145–1208), and human DGKη2–SAMD (amino acid residues 1151–1214) were amplified by PCR using KOD-plus DNA polymerase (Toyobo, Osaka, Japan) from the mouse testis cDNA or the plasmids we prepared as described above. The products were subcloned into the plasmids pGEX-6P-1 (GE Healthcare), p3×FLAG-CMV, pAcGFP-C1, or pCold-TF (Clontech-Takara Bio) at the EcoRI/SalI or BamHI/SalI site. pCold-TF is a fusion cold-shock expression vector, which expresses a hexahistidine (6×His)-tagged trigger factor (TF).

Expression and purification of GST-fusion proteins

To express GST-fused SMS1–SAMD (GST–SMS1–SAMD), SMSr–SAMD (GST–SMSr–SAMD), and GST alone, pGEX-6P-1-SMS1–SAMD, pGEX-6P-1-SMSr–SAMD, and pGEX-6P-1 alone were introduced into *E. coli* BL21 cells. GST–SMS1–SAMD and GST alone were expressed with 0.1 mM isopropyl 1-thio-β-D-galactopyranoside (IPTG) at 37 °C for 3 h in BL21 cells. GST–SMSr–SAMD was expressed with 0.1 mM IPTG at 18 °C for 16 h. The cells were harvested by centrifugation (15,000 × *g*, 20 min at 4 °C). The cell pellets were lysed in sonication buffer (PBS without potassium, pH 7.4, containing 1 mM dithiothreitol (DTT) and 1 mM phenylmethylsulfonyl fluoride (PMSF)). After sonication, the insoluble material was removed by centrifugation (15,000 × *g*, 20 min at 4 °C). The resultant supernatants were filtered through a 0.45-μm filter (Millipore. Tokyo, Japan). The GST-tagged proteins were purified by affinity chromatography on a GSH-Sepharose 4B column (GE Healthcare). The beads were washed once with sonication buffer, followed by washing with wash buffer (20 mM Tris-HCl, pH 7.5, 2 M NaCl). The GST-fused proteins were eluted with elution buffer A (PBS without potassium, pH 7.4, containing 5 mM GSH), followed by elution with elution buffer B (50 mM Tris-HCl, pH 9.6, containing 15 mM GSH). The purified proteins were dialyzed in PBS without potassium.

Expression and purification of 6×His–TF-fusion proteins

BL21 cells that harbored expression plasmids encoding 6×His–TF alone or 6×His–TF–DGKδ2–SAMD were grown at 37 °C in LB medium supplemented with 100 μg/ml ampicillin until the cell density reached an OD_{600} of 0.45. The cells were incubated at 16 °C for 24 h in the presence of 0.1 mM IPTG and then were harvested by centrifugation. The pellets were lysed by sonication on ice with a lysis buffer (50 mM sodium phosphate, pH 8.0, containing 500 mM NaCl, 1 mM PMSF, 1 mM DTT, 20 mg/ml aprotinin, 20 mg/ml leupeptin, 20 mg/ml pepstatin, and 1 mM soybean trypsin inhibitor) followed by centrifugation (15,000 × *g* for 40 min at 4 °C). Ammonium sulfate was added gradually to the supernatant to 40% saturation and incubated at 4 °C for 1 h with shaking. After centrifugation (15,000 × *g* for 45 min at 4 °C), the precipitates were removed, and the ammonium sulfate concentration in the remaining supernatants was further increased to 80% saturation. After 2 h of incubation at 4 °C with continuous shaking, precipitated proteins were collected by centrifugation (15,000 × *g* for 45 min at 4 °C), resuspended in 1 ml of 50 mM sodium phosphate, pH 8.0, and dialyzed in buffer (25 mM Tris-HCl, pH 8.0, 500 mM NaCl). The dialyzed proteins were purified by affinity chromatography on a Ni-Sepharose 6 Fast Flow column (GE Healthcare). The beads were washed with 30 ml of wash buffer (50 mM imidazole, 50 mM sodium phosphate, pH 8.0, 300 mM NaCl). Subsequently, the bound proteins were eluted with elution buffer (500 mM imidazole, 50 mM sodium phosphate, pH 8.0, 300 mM NaCl). The purified proteins were dialyzed in a buffer (20 mM sodium phosphate, pH 8.0, 150 mM NaCl).

GST-pulldown assay

GSH-Sepharose 4B (20 μl) was washed with lysis buffer (20 mM Tris-HCl, pH 7.5, 150 mM NaCl, 1 mM EDTA, 0.5% Triton X-100, and 1 mM PMSF). Purified GST-fused protein (20 μg) was incubated with beads in 300 μl of PBS at 4 °C for 30 min. Subsequently, beads were washed with lysis buffer four times,

and then 300 μl of PBS and 20 μg of 6×His–TF-fused protein was added. Beads and proteins were incubated at 4 °C for 2 h. Then the beads were washed with lysis buffer four times, and the proteins were eluted in 50 μl of 2× SDS sample buffer by incubation at 95 °C for 10 min.

Cell culture and transfection

COS-7 cells were maintained on 150-mm dishes (Thermo Fisher Scientific) in Dulbecco's modified Eagle's medium (DMEM) (Wako Pure Chemicals, Tokyo, Japan) containing 10% fetal bovine serum (FBS) (Thermo Fisher Scientific), 100 units/ml penicillin G (Wako Pure Chemicals), and 100 μg/ml streptomycin (Wako Pure Chemicals) at 37 °C in an atmosphere containing 5% CO_2. Cells (5×10^5) were plated on poly-L-lysine–coated 60-mm dishes for immunoprecipitation analysis. For quantitation of PA and DG levels, 1×10^6 cells were plated on 100-mm dishes. For confocal microscopy, 1.5×10^4 cells were plated on poly-L-lysine (Sigma)-coated glass coverslips (15 mm diameter). After 24 h, plasmid cDNAs were transfected using PolyFect (Qiagen) according to the manufacturer's instruction manual. After transfection, the cells were cultured for an additional 24 h and were used for the experiments described below.

Co-immunoprecipitation analysis

COS-7 cells co-expressing FLAG-tagged and V5-tagged proteins were washed two times with PBS and lysed in a buffer containing 50 mM HEPES, pH 7.4, 150 mM NaCl, 1 mM EDTA, 1% Nonidet P-40, 1 mM PMSF, and Complete EDTA-free protease inhibitor mixture (Roche Diagnostics, Mannheim, Germany). After sonication, insoluble materials were removed by centrifugation (10,000 × *g* for 5 min at 4 °C). Anti-V5 (1.5 μg) or anti-FLAG (5 μl) antibody was added to the cell lysates (400 μl). After a 2-h incubation at 4 °C, 20 μl of protein A/G PLUS-agarose beads (Santa Cruz Biotechnology, catalog no. sc-2003) was added and further incubated at 4 °C for 2 h. The beads were then washed five times with a wash buffer (50 mM HEPES, pH 7.4, 100 mM NaCl, 5 mM $MgCl_2$, 0.1% Triton X-100, 1 mM PMSF, 1 mM EDTA, and Complete EDTA-free protease inhibitor mixture). Co-immunoprecipitated proteins were eluted in 50 μl of 2× SDS sample buffer by incubation at 95 °C for 10 min.

Lipid extraction

Total lipids were extracted from the samples according to the method of Bligh and Dyer (43) as described previously (36, 44). Briefly, 2 ml of methanol and 1 ml of chloroform were added to 700 μl of sample. Internal standards (100 ng of the 14:0/14:0-PA (Avanti Polar Lipids) and 50 ng of the 14:0/14:0-DG (Cayman Chemical)) were added. To improve recovery ratio of acidic phospholipids, 100 μl of 3 M HCl was added to the sample. After addition of HCl, the sample was vortexed for 30 s. After incubation for 30 min at room temperature, 1 ml of chloroform was added and vortexed for 30 s, followed by the addition of 1 ml of water and vortexing for 30 s. The sample was centrifuged at 1000 × *g* for 10 min to separate the phases. The lower phase, containing the extracted lipids, was transferred to a new vial. The solvent-containing lipids was dried under N_2 gas, and the extracted lipids were reconstituted in 100 μl of chloroform/methanol (2:1, v/v).

Liquid chromatography

The extracted lipids (10 μl) were separated on a liquid chromatography (LC) system (EXION LC, AB SCIEX, Framingham, MA). This LC system was controlled by the Analys® software (AB SCIEX).

For detection of PA molecular species, PA molecular species were separated using UK-Silica column (3 μm, 150 × 2.0-mm inner diameter, Imtakt, Kyoto, Japan) as described previously (36, 45, 46). A binary gradient consisting of two solvents: solvent A (chloroform/methanol (89:10) containing 0.28% ammonia) and solvent B (chloroform/methanol/water (55:39:5) containing 0.28% ammonia) were used. The gradient elution program was 20% B for 5 min, 20–30% B for 10 min, 30–60% B for 25 min, 60% B for 5 min, 60–20% B for 1 min, followed by 20% B for 14 min. The flow rate was 0.3 ml/min, and chromatography was performed at 25 °C.

For detection of DG molecular species, DG molecular species were separated using UK-C18 column (3 μm, 150 × 3.0-mm inner diameter, Imtakt) as described (47) with a modification. A binary gradient consisting of two solvents: solvent A (chloroform/methanol/water (50:220:70) containing 1 mM ammonium acetate) and solvent B (hexane/chloroform/methanol (70:130:100) containing 1 mM ammonium acetate) were used. The gradient elution program was 25% B for 15 min, 25–60% B for 25 min, 60–75% B for 3 min, 75–100% B for 5 min, 100% B for 10 min, 100–25% B for 1 min followed by 25% B for 5 min. The flow rate was 0.2 ml/min, and chromatography was performed at 25 °C.

Mass spectrometry

The LC system was coupled on line to Triple Quad™ 4500 (AB SCIEX), a triple-quadrupole tandem mass spectrometer equipped with a turbo spray ionization source. The experimental conditions for detection of PA molecular species were as follows: ion spray voltage −4500 V, curtain gas 30 p.s.i., collision gas 6 p.s.i., temperature 300 °C, declustering potential −160 V, entrance potential −10 V, collision energy −42 V, collision cell exit potential −11 V, ion source gas I 70 p.s.i., and ion source gas II 30 p.s.i.. The experimental conditions for detection of DG molecular species were as follows: ion spray voltage 5500 V, curtain gas 30 p.s.i., collision gas 7 p.s.i., temperature 300 °C, declustering potential 60 V, entrance potential 10 V, collision energy 30 V, collision cell exit potential 6.0 V, ion source gas I 70 p.s.i., and ion source gas II 50 p.s.i.

PA and DG molecular species were detected in a multiple reaction monitoring mode. Ionized PA species ($[M - H]^-$) or DG species ($[M + NH_4]^+$) were isolated at the first quadrupole (Q1). Thereafter, a product ion of PA species (*m*/*z* 153 in negative ion mode) (48, 49) or DG species (see Tables S1 and S2) was reselected at Q3 after fragmentation at Q2 by collision-induced dissociation.

Expression and purification of 6×His-tagged human DGKδ2 and SMSr

pSF-CMV-NH_2-His-EKT3-DGKδ2, -SMSr, or -SMSr–ΔSAMD were transfected into COS-7 cells by electroporation using the Gene Pulser Xcell™ electroporation system (Bio-Rad, Tokyo, Japan), as described previously (50). The transfected cells were then allowed to grow for 48 h in Dulbecco's modified Eagle's medium containing 10% FBS.

The cells (10 dishes 150 mm in diameter) were harvested and lysed by sonication on ice with lysis buffer (50 mM sodium phosphate, pH 8.0, 1% Triton X-100, 300 mM NaCl, 10 mM imidazole, 1 mM PMSF, 20 mg/ml aprotinin, 20 mg/ml leupeptin, 20 mg/ml pepstatin, and 1 mM soybean trypsin inhibitor) followed by centrifugation at 15,000 × *g* at 4 °C for 40 min. The lysate was filtered through a 0.45-μm filter (Millipore). The proteins were purified by affinity chromatography on a Ni-Sepharose 6 Fast Flow column (GE Healthcare). The beads were washed once with lysis buffer, followed by washing with wash buffer (50 mM sodium phosphate, pH 8.0, 50 mM imidazole, 300 mM NaCl). 6×His-tagged proteins were eluted with elution buffer (50 mM sodium phosphate, pH 8.0, 300 mM imidazole, 300 mM NaCl). The purified proteins were used for *in vitro* DGK assays described below.

In vitro DGK assay

DGKδ2 activity was measured using an octyl-β-D-glucoside–mixed micellar assay (26), followed by quantitation of PA levels using LC-MS/MS as described above. In brief, 100 μl of purified proteins, prepared as described above, were used for the assay. The enzyme reaction was started by adding 150 μl of reaction solution containing the final concentration of 50 mM MOPS, pH 7.4, 20 mM NaF, 10 mM $MgCl_2$, 50 mmol/liter *n*-octyl-β-D-glucoside, 1 mM DTT, 1 mM (1.96 mol %) 16:0/18:1-DG (Avanti Polar Lipids), and 0.2 mM ATP. The solution was incubated at 37 °C for 2 h. After the reaction, lipids were extracted as described above. The 34:1-PA in the extracted lipids was detected by LC-MS/MS as described above. The DGK assay was also performed using the ADP-Glo kinase assay kit as described previously (26).

Immunoblot analysis

Proteins eluted in an SDS sample buffer were separated by SDS-PAGE. The separated proteins were transferred to a polyvinylidene difluoride membrane (Wako) and blocked with 5% skim milk in TBS-T (10 mM Tris-HCl, pH 7.4, 150 mM NaCl, 0.05% (v/v) Tween 20) for 1 h at room temperature. After washing with TBS-T, the membrane was incubated with an antibody in 5% BSA in TBS-T for 16 h at 4 °C. The immunoreactive bands were then visualized using a peroxidase-conjugated IgG antibody and the enhanced chemiluminescence Western blotting detection system (GE Healthcare).

Statistical analysis

Data are represented as the means ± S.D. and were analyzed using the Student's *t* test for the comparison of two groups or one-way analysis of variance followed by Tukey's post hoc test for multiple comparisons using GraphPad Prism 8 (GraphPad) to determine any significant differences. $p < 0.05$ was considered significant.

Author contributions—C. M. and F. S. conceptualization; C. M. and F. S. funding acquisition; C. M. and F. H. investigation; C. M. and F. S. writing-original draft; C. M., F. H., H. S., Y. H., A. Y., and F. S. writing-review and editing; H. S., Y. H., and A. Y. resources; H. S., Y. H., and A. Y. methodology; F. S. supervision; F. S. project administration.

References

1. Sakane, F., Mizuno, S., Takahashi, D., and Sakai, H. (2018) Where do substrates of diacylglycerol kinases come from? Diacylglycerol kinases utilize diacylglycerol species supplied from phosphatidylinositol turnover-independent pathways. *Adv. Biol. Regul.* **67,** 101–108 CrossRef Medline
2. Mérida, I., Avila-Flores, A., and Merino, E. (2008) Diacylglycerol kinases: at the hub of cell signalling. *Biochem. J.* **409,** 1–18 CrossRef Medline
3. Topham, M. K., and Epand, R. M. (2009) Mammalian diacylglycerol kinases: molecular interactions and biological functions of selected isoforms. *Biochim. Biophys. Acta* **1790,** 416–424 CrossRef Medline
4. Sakane, F., Imai, S., Kai, M., Yasuda, S., and Kanoh, H. (2007) Diacylglycerol kinases: why so many of them? *Biochim. Biophys. Acta* **1771,** 793–806 CrossRef Medline
5. Goto, K., Hozumi, Y., and Kondo, H. (2006) Diacylglycerol, phosphatidic acid, and the converting enzyme, diacylglycerol kinase, in the nucleus. *Biochim. Biophys. Acta* **1761,** 535–541 CrossRef Medline
6. Nishizuka, Y. (1992) Intracellular signaling by hydrolysis of phospholipids and activation of protein kinase C. *Science* **258,** 607–614 CrossRef Medline
7. Ebinu, J. O., Bottorff, D. A., Chan, E. Y., Stang, S. L., Dunn, R. J., and Stone, J. C. (1998) RasGRP, a Ras guanyl nucleotide–releasing protein with calcium- and diacylglycerol-binding motifs. *Science* **280,** 1082–1086 CrossRef Medline
8. Massart, J., and Zierath, J. R. (2019) Role of diacylglycerol kinases in glucose and energy homeostasis. *Trends Endocrinol. Metab.* **30,** 603–617 CrossRef Medline
9. Miele, C., Paturzo, F., Teperino, R., Sakane, F., Fiory, F., Oriente, F., Ungaro, P., Valentino, R., Beguinot, F., and Formisano, P. (2007) Glucose regulates diacylglycerol intracellular levels and protein kinase C activity by modulating diacylglycerol kinase subcellular localization. *J. Biol. Chem.* **282,** 31835–31843 CrossRef Medline
10. Schmitz-Peiffer, C., Browne, C. L., Oakes, N. D., Watkinson, A., Chisholm, D. J., Kraegen, E. W., and Biden, T. J. (1997) Alterations in the expression and cellular localization of protein kinase C isozymes epsilon and theta are associated with insulin resistance in skeletal muscle of the high-fat-fed rat. *Diabetes* **46,** 169–178 CrossRef Medline
11. Avignon, A., Yamada, K., Zhou, X., Spencer, B., Cardona, O., Saba-Siddique, S., Galloway, L., Standaert, M. L., and Farese, R. V. (1996) Chronic activation of protein kinase C in soleus muscles and other tissues of insulin-resistant type II diabetic Goto-Kakizaki (GK), obese/aged, and obese/Zucker rats. A mechanism for inhibiting glycogen synthesis. *Diabetes* **45,** 1396–1404 CrossRef Medline
12. Heydrick, S. J., Ruderman, N. B., Kurowski, T. G., Adams, H. B., and Chen, K. S. (1991) Enhanced stimulation of diacylglycerol and lipid synthesis by insulin in denervated muscle. Altered protein kinase C activity and possible link to insulin resistance. *Diabetes* **40,** 1707–1711 CrossRef Medline
13. Yu, C., Chen, Y., Cline, G. W., Zhang, D., Zong, H., Wang, Y., Bergeron, R., Kim, J. K., Cushman, S. W., Cooney, G. J., Atcheson, B., White, M. F., Kraegen, E. W., and Shulman, G. I. (2002) Mechanism by which fatty acids inhibit insulin activation of insulin receptor substrate-1 (IRS-1)-associated phosphatidylinositol 3-kinase activity in muscle. *J. Biol. Chem.* **277,** 50230–50236 CrossRef Medline
14. Chibalin, A. V., Leng, Y., Vieira, E., Krook, A., Björnholm, M., Long, Y. C., Kotova, O., Zhong, Z., Sakane, F., Steiler, T., Nylén, C., Wang, J., Laakso, M., Topham, M. K., Gilbert, M., Wallberg-Henriksson, H., and Zierath, J. R. (2008) Downregulation of diacylglycerol kinase δ contributes to hy-

perglycemia-induced insulin resistance. *Cell* **132,** 375–386 CrossRef Medline
15. Sakai, H., Kado, S., Taketomi, A., and Sakane, F. (2014) Diacylglycerol kinase δ phosphorylates phosphatidylcholine-specific phospholipase C-dependent, palmitic acid-containing diacylglycerol species in response to high glucose levels. *J. Biol. Chem.* **289,** 26607–26617 CrossRef Medline
16. Dahanukar, A., Walker, J. A., and Wharton, R. P. (1999) Smaug, a novel RNA-binding protein that operates a translational switch in *Drosophila*. *Mol. Cell* **4,** 209–218 CrossRef Medline
17. Barrera, F. N., Poveda, J. A., González-Ros, J. M., and Neira, J. L. (2003) Binding of the C-terminal sterile α motif (SAM) domain of human p73 to lipid membranes. *J. Biol. Chem.* **278,** 46878–46885 CrossRef Medline
18. Sakai, H., and Sakane, F. (2012) Recent progress on type II diacylglycerol kinases: the physiological functions of diacylglycerol kinase δ, η, and κ and their involvement in disease. *J. Biochem.* **152,** 397–406 CrossRef Medline
19. Murakami, T., Sakane, F., Imai, S., Houkin, K., and Kanoh, H. (2003) Identification and characterization of two splice variants of human diacylglycerol kinase η. *J. Biol. Chem.* **278,** 34364–34372 CrossRef Medline
20. Imai, S., Sakane, F., and Kanoh, H. (2002) Phorbol ester-regulated oligomerization of diacylglycerol kinase δ linked to its phosphorylation and translocation. *J. Biol. Chem.* **277,** 35323–35332 CrossRef Medline
21. Sakane, F., Imai, S., Yamada, K., Murakami, T., Tsushima, S., and Kanoh, H. (2002) Alternative splicing of the human diacylglycerol kinase 8 gene generates two isoforms differing in their expression patterns and in regulatory functions. *J. Biol. Chem.* **277,** 43519–43526 CrossRef Medline
22. Cabukusta, B., Kol, M., Kneller, L., Hilderink, A., Bickert, A., Mina, J. G., Korneev, S., and Holthuis, J. C. (2017) ER residency of the ceramide phosphoethanolamine synthase SMSr relies on homotypic oligomerization mediated by its SAM domain. *Sci. Rep.* **7,** 41290 CrossRef Medline
23. Cabukusta, B., Köhlen, J. A., Richter, C. P., You, C., and Holthuis, J. C. (2016) Monitoring changes in the oligomeric state of a candidate endoplasmic reticulum (ER) ceramide sensor by single-molecule photobleaching. *J. Biol. Chem.* **291,** 24735–24746 CrossRef Medline
24. Vacaru, A. M., Tafesse, F. G., Ternes, P., Kondylis, V., Hermansson, M., Brouwers, J. F., Somerharju, P., Rabouille, C., and Holthuis, J. C. (2009) Sphingomyelin synthase-related protein SMSr controls ceramide homeostasis in the ER. *J. Cell Biol.* **185,** 1013–1027 CrossRef Medline
25. Harada, B. T., Knight, M. J., Imai, S., Qiao, F., Ramachander, R., Sawaya, M. R., Gingery, M., Sakane, F., and Bowie, J. U. (2008) Regulation of enzyme localization by polymerization: polymer formation by the SAM domain of diacylglycerol kinase δ1. *Structure* **16,** 380–387 CrossRef Medline
26. Sato, M., Liu, K., Sasaki, S., Kunii, N., Sakai, H., Mizuno, H., Saga, H., and Sakane, F. (2013) Evaluations of the selectivities of the diacylglycerol kinase inhibitors R59022 and R59949 among diacylglycerol kinase isozymes using a new non-radioactive assay method. *Pharmacology* **92,** 99–107 CrossRef Medline
27. Qiao, F., and Bowie, J. U. (2005) The many faces of SAM. *Science's STKE* **2005,** re7 CrossRef Medline
28. Rajakulendran, T., Sahmi, M., Kurinov, I., Tyers, M., Therrien, M., and Sicheri, F. (2008) CNK and HYP form a discrete dimer by their SAM domains to mediate RAF kinase signaling. *Proc. Natl. Acad. Sci. U.S.A.* **105,** 2836–2841 CrossRef Medline
29. Leone, M., Cellitti, J., and Pellecchia, M. (2008) NMR studies of a heterotypic Sam–Sam domain association: the interaction between the lipid phosphatase Ship2 and the EphA2 receptor. *Biochemistry* **47,** 12721–12728 CrossRef Medline
30. Kol, M., Panatala, R., Nordmann, M., Swart, L., van Suijlekom, L., Cabukusta, B., Hilderink, A., Grabietz, T., Mina, J. G. M., Somerharju, P., Korneev, S., Tafesse, F. G., and Holthuis, J. C. M. (2017) Switching head group selectivity in mammalian sphingolipid biosynthesis by active-site-engineering of sphingomyelin synthases. *J. Lipid Res.* **58,** 962–973 CrossRef Medline
31. Sakane, F., Imai, S., Kai, M., Wada, I., and Kanoh, H. (1996) Molecular cloning of a novel diacylglycerol kinase isozyme with a pleckstrin homology domain and a C-terminal tail similar to those of the EPH family of protein-tyrosine kinases. *J. Biol. Chem.* **271,** 8394–8401 CrossRef Medline
32. Ogushi, F., Ishitsuka, R., Kobayashi, T., and Sugita, Y. (2012) Rapid flip-flop motions of diacylglycerol and ceramide in phospholipid bilayers. *Chem. Phys. Lett.* **522,** 96–102 CrossRef
33. Uchida, Y., Hasegawa, J., Chinnapen, D., Inoue, T., Okazaki, S., Kato, R., Wakatsuki, S., Misaki, R., Koike, M., Uchiyama, Y., Iemura, S., Natsume, T., Kuwahara, R., Nakagawa, T., Nishikawa, K., *et al.* (2011) Intracellular phosphatidylserine is essential for retrograde membrane traffic through endosomes. *Proc. Natl. Acad. Sci. U.S.A.* **108,** 15846–15851 CrossRef Medline
34. Bickert, A., Ginkel, C., Kol, M., vom Dorp, K., Jastrow, H., Degen, J., Jacobs, R. L., Vance, D. E., Winterhager, E., Jiang, X. C., Dörmann, P., Somerharju, P., Holthuis, J. C., and Willecke, K. (2015) Functional characterization of enzymes catalyzing ceramide phosphoethanolamine biosynthesis in mice. *J. Lipid Res.* **56,** 821–835 CrossRef Medline
35. Usuki, T., Sakai, H., Shionoya, T., Sato, N., and Sakane, F. (2015) Expression and localization of type II diacylglycerol kinase isozymes δ and η in the developing mouse brain. *J. Histochem. Cytochem.* **63,** 57–68 CrossRef Medline
36. Komenoi, S., Suzuki, Y., Asami, M., Murakami, C., Hoshino, F., Chiba, S., Takahashi, D., Kado, S., and Sakane, F. (2019) Microarray analysis of gene expression in the diacylglycerol kinase η knockout mouse brain. *Biochem. Biophys. Rep.* **19,** 100660 CrossRef Medline
37. Hayashi, Y., Nemoto-Sasaki, Y., Matsumoto, N., Hama, K., Tanikawa, T., Oka, S., Saeki, T., Kumasaka, T., Koizumi, T., Arai, S., Wada, I., Yokoyama, K., Sugiura, T., and Yamashita, A. (2018) Complex formation of sphingomyelin synthase 1 with glucosylceramide synthase increases sphingomyelin and decreases glucosylceramide levels. *J. Biol. Chem.* **293,** 17505–17522 CrossRef Medline
38. Hayashi, Y., Nemoto-Sasaki, Y., Tanikawa, T., Oka, S., Tsuchiya, K., Zama, K., Mitsutake, S., Sugiura, T., and Yamashita, A. (2014) Sphingomyelin synthase 2, but not sphingomyelin synthase 1, is involved in HIV-1 envelope-mediated membrane fusion. *J. Biol. Chem.* **289,** 30842–30856 CrossRef Medline
39. Hayashi, Y., Nemoto-Sasaki, Y., Matsumoto, N., Tanikawa, T., Oka, S., Tanaka, Y., Arai, S., Wada, I., Sugiura, T., and Yamashita, A. (2017) Carboxyl-terminal tail-mediated homodimerizations of sphingomyelin synthases are responsible for efficient export from the endoplasmic reticulum. *J. Biol. Chem.* **292,** 1122–1141 CrossRef Medline
40. Imai, S., Yasuda, S., Kai, M., Kanoh, H., and Sakane, F. (2009) Diacylglycerol kinase δ associates with receptor for activated C kinase 1, RACK1. *Biochim. Biophys. Acta* **1791,** 246–253 CrossRef Medline
41. Takeuchi, M., Sakiyama, S., Usuki, T., Sakai, H., and Sakane, F. (2012) Diacylglycerol kinase δ1 transiently translocates to the plasma membrane in response to high glucose. *Biochim. Biophys. Acta* **1823,** 2210–2216 CrossRef Medline
42. Murakami, E., Shionoya, T., Komenoi, S., Suzuki, Y., and Sakane, F. (2016) Cloning and characterization of novel testis-specific diacylglycerol kinase η splice variants 3 and 4. *PLoS ONE* **11,** e0162997 CrossRef Medline
43. Bligh, E. G., and Dyer, W. J. (1959) A rapid method of total lipid extraction and purification. *Can. J. Biochem. Physiol.* **37,** 911–917 CrossRef Medline
44. Honda, S., Murakami, C., Yamada, H., Murakami, Y., Ishizaki, A., and Sakane, F. (2019) Analytical method for diacylglycerol kinase ζ activity in cells using protein myristoylation and liquid chromatography-tandem mass spectrometry. *Lipids* **54,** 763–771 CrossRef Medline
45. Yamaki, A., Akiyama, R., Murakami, C., Takao, S., Murakami, Y., Mizuno, S., Takahashi, D., Kado, S., Taketomi, A., Shirai, Y., Goto, K., and Sakane, F. (2019) Diacylglycerol kinase α-selective inhibitors induce apoptosis and reduce viability of melanoma and several other cancer cell lines. *J. Cell Biochem.* **120,** 10043–10056 CrossRef Medline
46. Mizuno, S., Sakai, H., Saito, M., Kado, S., and Sakane, F. (2012) Diacylglycerol kinase-dependent formation of phosphatidic acid molecular species during interleukin-2 activation in CTLL-2 T-lymphocytes. *FEBS Open Bio* **2,** 267–272 CrossRef Medline
47. Murakami, C., Mizuno, S., Kado, S., and Sakane, F. (2017) Development of a liquid chromatography-mass spectrometry based enzyme activity assay for phosphatidylcholine-specific phospholipase C. *Anal. Biochem.* **526,** 43–49 CrossRef Medline

48. Fang, N., Yu, S., and Badger, T. M. (2003) LC-MS/MS analysis of lysophospholipids associated with soy protein isolate. *J. Agric. Food Chem.* **51,** 6676–6682 CrossRef Medline
49. Okudaira, M., Inoue, A., Shuto, A., Nakanaga, K., Kano, K., Makide, K., Saigusa, D., Tomioka, Y., and Aoki, J. (2014) Separation and quantification of 2-acyl-1-lysophospholipids and 1-acyl-2-lysophospholipids in biological samples by LC-MS/MS. *J. Lipid Res.* **55,** 2178–2192 CrossRef Medline
50. Sato, Y., Murakami, C., Yamaki, A., Mizuno, S., Sakai, H., and Sakane, F. (2016) Distinct 1-monoacylglycerol and 2-monoacylglycerol kinase activities of diacylglycerol kinase isozymes. *Biochim. Biophys. Acta* **1864,** 1170–1176 CrossRef Medline
51. Chenna, R., Sugawara, H., Koike, T., Lopez, R., Gibson, T. J., Higgins, D. G., and Thompson, J. D. (2003) Multiple sequence alignment with the Clustal series of programs. *Nucleic Acids Res.* **31,** 3497–3500 CrossRef Medline
52. Thompson, J. D., Higgins, D. G., and Gibson, T. J. (1994) CLUSTAL W: improving the sensitivity of progressive multiple sequence alignment through sequence weighting, position-specific gap penalties and weight matrix choice. *Nucleic Acids Res.* **22,** 4673–4680 CrossRef Medline